

**The potential for using geomagnetic data
as proxy for river discharge into the
Arctic and a review of other
potential proxies**

**Robert Tyler
C²GCR Report No. 92-16
October 1992**

The Potential for Using Geomagnetic Data
as Proxy for River Discharge into the Arctic
and a Review of Other Potential Proxies

Robert Tyler

October 16, 1992

Department of Atmospheric and Oceanic Sciences
and
Center for Climate and Global Change Research
McGill University
805 Sherbrooke St. W.
Montreal, Quebec

Abstract

Considerable attention has recently been directed toward studying the role of river runoff in Arctic sea-ice concentration, convective overturning in the Iceland Sea and climate in the Northern North Atlantic. In particular, variations in the MacKenzie River runoff may play an important role in an interdecadal Arctic climate cycle. Here we present the record of measured MacKenzie runoff and discuss the potential of other data sources that can be used as proxy. Reasonable potential exists for extracting this runoff record from tree ring, ice, and sediment cores. However, there has not yet been an adequate number of cores taken from the appropriate locations.

Geomagnetic records from Cambridge Bay in the Canadian Arctic are shown to be well correlated with MacKenzie runoff. Monthly transport through the Bering Strait is shown to be correlated with the geomagnetic record at Barrows Alaska. We discuss the physical mechanisms that appear to explain these correlations and propose that geomagnetic data may be used to both extend and complement records of river discharge and freshwater transport in the sea.

Contents

1	Introduction	1
2	Proxy Data	3
2.1	Tree Rings	3
2.2	Ice Cores	9
2.3	Sediment Record	17
2.4	Historical Data Using Content Analysis	20
3	Motionally-Induced Electromagnetic Fields in the Sea (MIEFS)	21
3.1	Theoretical Considerations	24
3.2	Magnetic Observations	33
4	Summary	42
5	Acknowledgements	47
6	References	47

List of Figures

1	North American drainage basin	2
2	MacKenzie River discharge	4
3	Discharge at Norman Wells	5
4	Total Arctic discharge from North America	6
5	Tree rings	7
6	Location of trees used in Lake Athabasca Reconstruction	10
7	Tree series from the Peace-Athabasca Delta	11
8	Reconstruction of water-level record of Lake Athabasca	12
9	Koch ice-severity index	13
10	Percent ice melt on Agassiz Ice Cap	15
11	ΔO^{18} and ice accumulation on Agassiz Ice Cap	16
12	Cross-correlation of Agassiz ice accumulation and the Koch index	18
13	Glacial mass balance in British Columbia	19
14	Historical record at Albany, Ontario	22
15	Correlations of Albany winter length with Agassiz ΔO^{18} and the Koch ice index	23
16	Idealized ocean flow for motionally-induced electromagnetic fields in the sea (MIEFS)	25
17	Ocean conductivity typical of globe	28
18	Ocean conductivity typical of Arctic	29
19	Coordinate system used in geomagnetic studies	31
20	Map showing locations of magnetic observatories	34
21	Time rate of change of magnetic intensity at Cambridge Bay (CBB)	36
22	Magnetic Observations at Resolute Bay (RES) and North American Runoff	38
23	Monthly Transport through Bering Strait	40
24	Monthly average of available data from magnetic observatory at Barrows, Alaska	41
25	Magnetic Observations at Victoria, British Columbia	43
26	Magnetic Observations at Sitka, Alaska	44

1 Introduction

Recently, a considerable amount of scientific interest has been directed toward studying the role of high-latitude ocean dynamics in global climate. It has long been recognized that a decrease in polar air temperatures and the resultant increase in ice coverage (decrease in albedo) form a positive feedback loop with the potential for creating large global changes from small perturbations. Of more recent finding is that the stability of the oceanic *conveyor belt*, which transports heat poleward from the equator, may also be sensitive to certain high-latitude oceanographic processes. (See Weaver and Hughes (1992) for a review of the stability and variations in the thermohaline circulation.)

The thermohaline circulation (THC) is driven by deep water formation south of Iceland, a process which includes the sinking Denmark Strait overflow water from the Greenland and Iceland Seas. The water properties of the latter are affected by the rate of convection in this region during winter. Since the ocean water density is largely controlled by salinity (and secularly, temperature) at high latitudes, the magnitude of the outflow from the Arctic of ice and low-salinity water is very important in determining the water properties there.

Numerical studies suggests that small changes in the flux of freshwater into these areas (Greenland, Iceland and Labrador Seas) can result in large changes in the thermohaline circulation, possibly changing it from one mode into another mode (Manabe and Stouffer, 1988; Stocker and Wright, 1991).

Several investigators have recently stressed the importance of freshwater fluxes (in the form of ice) into these areas of deep convection (Mysak and Manak, 1989; Aagaard and Carmack 1989; Mysak et al. 1990) and the relation of Arctic river discharge to sea-ice and salinity anomalies (Cattle, 1985; Mysak and Power, 1991). Mysak and Power (1991) found that Greenland Sea ice anomalies are significantly lag-correlated with North American runoff into the Arctic. Even though the total discharge into the Arctic from the Eurasian continent is several times that of the discharge from North America, it is thought that the role of the North American runoff in bringing about sea-ice anomalies in the Greenland Sea and Central Arctic predominates since the very wide and shallow Eurasian shelf is expected to allow for considerable mixing of the fresh runoff with Central Arctic Ocean waters that rise up onto the shelf (Ikeda, 1990; Mysak, 1992).

We have discussed above that the predominant freshwater signal forcing sea-ice anomalies is due to North American runoff into the Arctic. Now we propose that the predominant signal in this runoff is due to the MacKenzie River. We shall see that for the drainage basin into the Arctic (figure 1 b), variations—at least over a season—are most pronounced in the western section of the basin which contributes to MacKenzie runoff. The eastern end of the drainage basin is

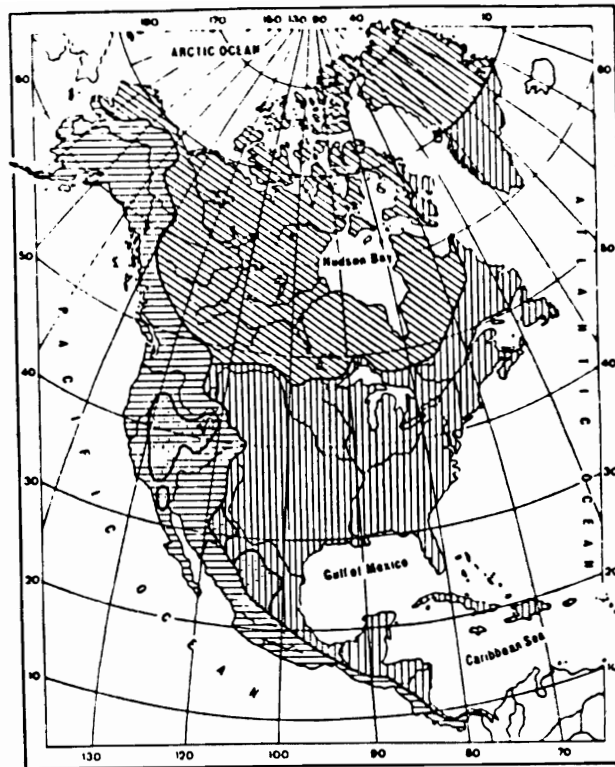


Fig. 71 Ocean drainage basins of North America.
 1 - Pacific; 2 - Atlantic; 3 - Arctic; 4 - internal drainage.

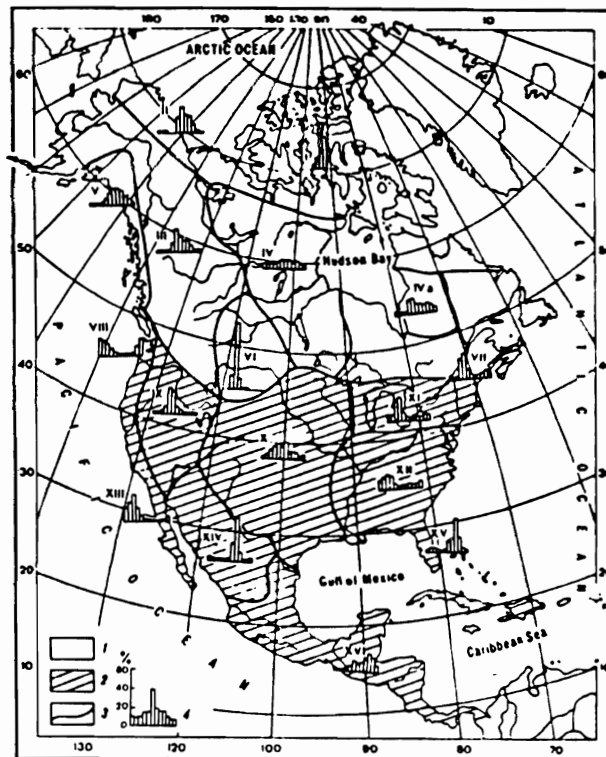


Fig. 74. Regions of North America with different annual run-off patterns
 1 - rivers with floods; 2 - rivers with a freshet cycle; 3 - boundaries of regions with the same annual run-off pattern; 4 - run-off hydrograph typical of the region

Figure 1: In (a) we see the drainage basin (area 3) used in calculating the time series shown in figure 4. In (b) the annual runoff patterns for the different areas are shown. Note that for the Arctic drainage basin (seen in (a)), the western part of the basin and the Archipelago contain sharp peaks in discharge while the discharge from the large rivers draining into the Hudson Bay are more constant. (Taken from Markova (1978).)

less mountainous and less directly connected to the Arctic Ocean. The result will be that freshwater signals from these areas will tend to be dampened because of the more sluggish drainage response and increased mixing. Hence, because of this and the arguments presented above, we propose that strong freshwater signals in the Arctic will be due primarily to MacKenzie river runoff.

Reliable estimates of the MacKenzie River runoff are only available for a period covering the last couple of decades (figure 2). In earlier measurements, gaps in the record and recording errors were more common. Since these gaps and errors were often associated with the spring break-up of ice, systematic errors may also have been included. Records involving earlier measurements such as those taken at Norman Wells (figure 3) are to be regarded with caution (Marsh, 1992).

In Markova (1978) an attempt has been made to combine historical measurements to obtain values for the total value of North American runoff into the Arctic. The resulting series (figure 4) stretches from 1918 to 1967.

However, this series relies on discontinuous and questionable early measurements and should be regarded with caution.

It seems then that there is a great need to both complement and extend the measured record of MacKenzie discharge with proxy sources. The possibilities of doing so are the subject of this report.

The report is organized as follows: In section 2 we review several conventional high-resolution proxy data sources and investigate possibilities for their use as proxy data for runoff; then, in section 3 we explore the possibility of using geomagnetic observations as indicators of discharge.

2 Proxy Data

2.1 Tree Rings

The use of tree rings for dating (dendrochronology) and as an indicator of climate (dendroclimatology) is now common (see the authoritative book by Fritz (1991) or Bradley (1985) for an excellent description). Briefly, a cross section of most trees from temperate forests reveal a pattern of alternating light and dark bands that reflect seasonal growth increments (see figure 5).

The light bands correspond to ‘early wood’ and the dark bands to ‘late wood’. The width of these annual pairs of light and dark bands (together considered a ring) are a function of many variables. The factors that are important in ring-width variations within a core include climatic processes—precipitation and temperature often being the most important.

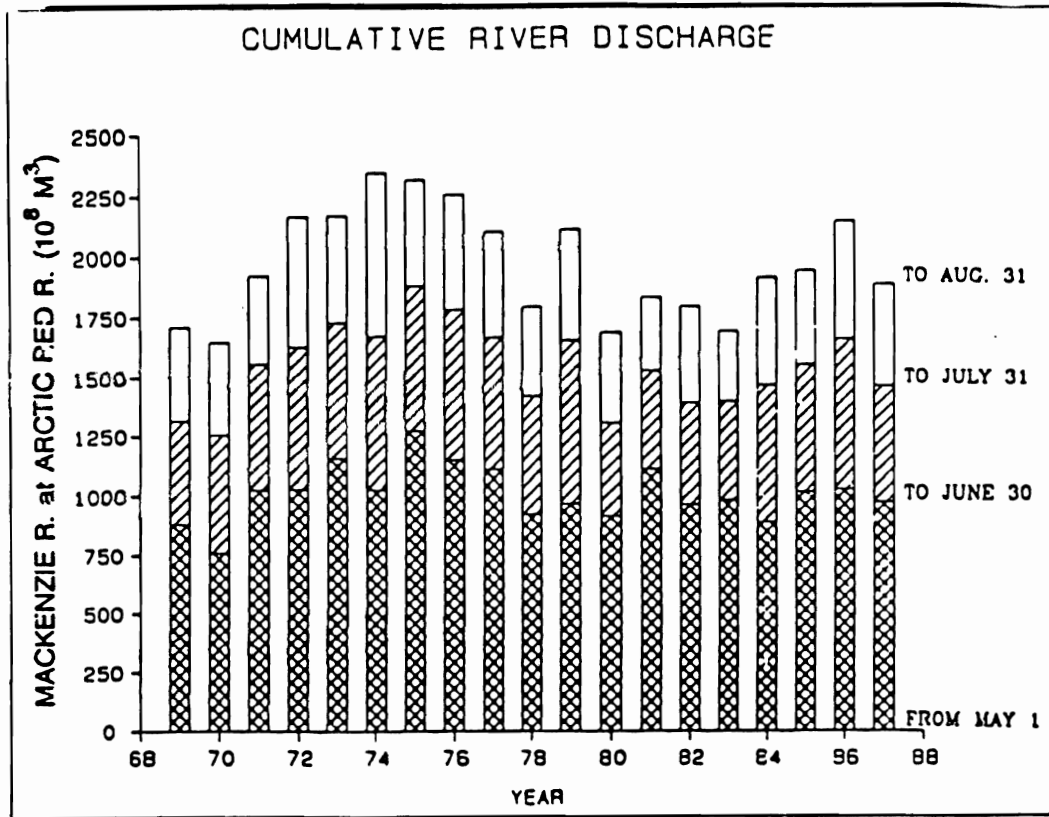


Figure 2: The cumulative volume discharge of the MacKenzie River (at Arctic Red River) for May-June, July and August. Taken from Fissel and Melling (1990).

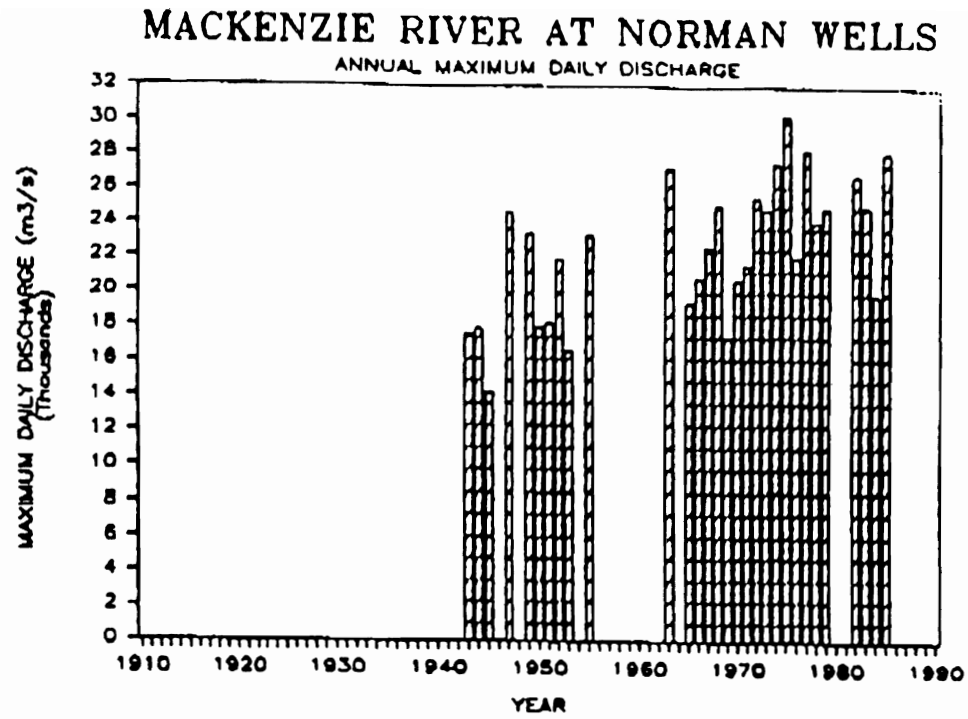


Figure 3: Annual averages of the maximum daily discharge at Norman Wells, Northwest Territories are plotted. Taken from Hirst et al. (1987).

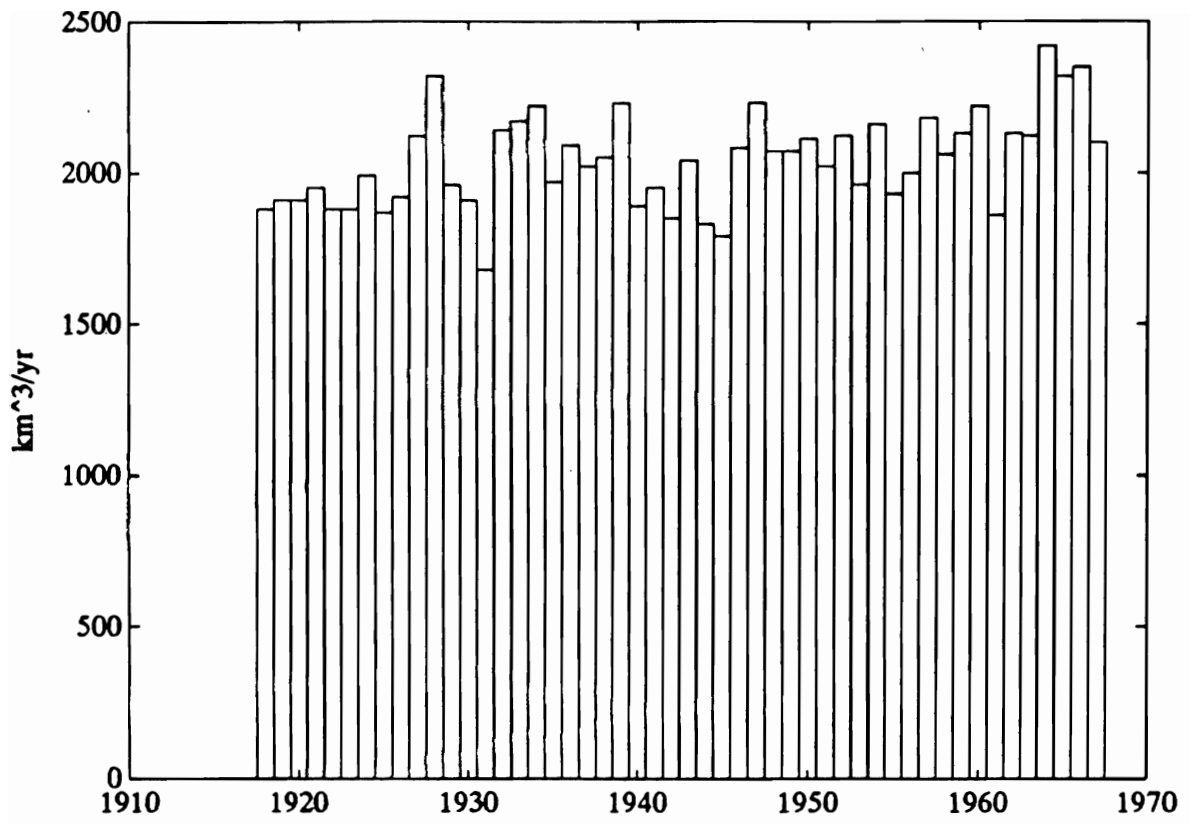


Figure 4: The discharge includes runoff into both the Arctic Ocean and Hudson Bay (see figure 1 (a)). Data taken from table in Markova (1978).

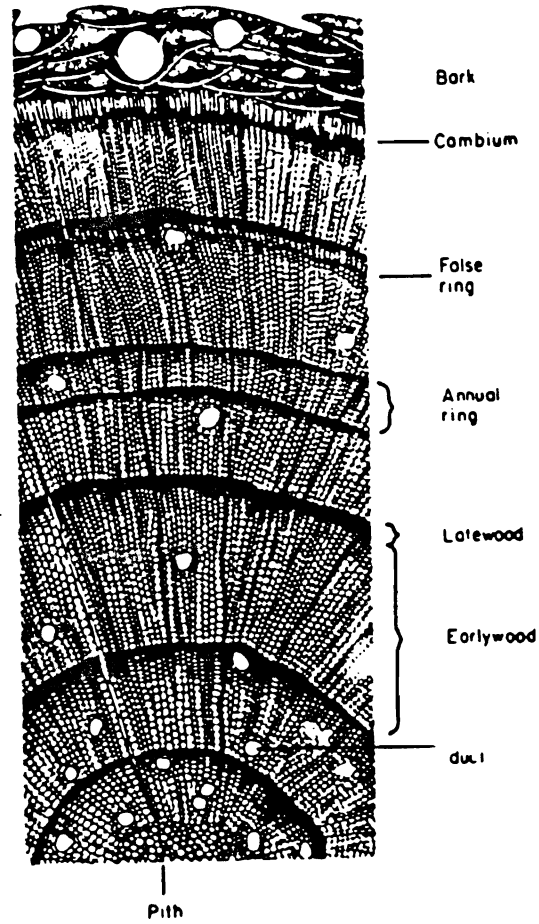


Figure 5: Shown is a drawing of the cell structure along a cross-section of a young stem of a conifer. The earlywood is made up of large relatively thin-walled cells; latewood is made up of small, thick-walled cells. Taken from Bradley (1985) (after Fritts (1976)).

Since tree trunks grow from the inside outward, a core taken from the tree reveals a record of tree growth with at least annual resolution. In order to isolate the climate signal from this core the rings must be standardized to account for greater growth during the younger stages. This is not a trivial task and as of yet no standardized method for doing this has been possible (Bradley, 1985). To increase the climate signal to noise ratio, trees are selected that are “under stress”, i.e., are growing close to their extreme geographical range. However, for dendroclimatic and isotope studies “complacent” trees are often preferred provided enough tree samples are available to isolate the climatic signal. Another method of amplifying the signal is performed by averaging over many standardized tree-ring sets.

Of interest here is whether tree rings can be used as proxy data for MacKenzie River discharge—this idea was originally suggested to us by S. Powers (1990, personal communication). There are a few ways in which we might imagine river runoff and tree growth to be related. For example, precipitation might be reflected in both river discharge as well as tree growth, provided the *local* precipitation variance is sufficiently crucial in tree growth. Implicit in the last statement is the following problem. Rivers—where their runoff values are described by precipitation—will be efficient integrators of both local and nonlocal precipitation. Trees, however, are usually¹ dependent on *local* precipitation. For this reason and others such as averaging that were already mentioned, there is probably a need to obtain many ring cores from a wide geographic area before this connection through precipitation can be pursued.

Another possible way in which MacKenzie runoff and tree growth might be related is through temperature variations. It is believed that the large region of MacKenzie drainage will contain both trees where precipitation is the limiting factor and—as we approach the arctic tree-line—trees where temperature becomes the limiting factor (R. D’Arrigo, 1992, personal communication). Since snow and ice melt will generally depend on temperature and this melt water would contribute to runoff, we see a possible connection between runoff and temperature-sensitive tree growth. However, again we have the problem of comparing local and nonlocal effects. Also, we would need to assume here that the runoff signal is carried predominantly in variations in melting quasi-perennial features such as glaciers rather than directly in levels of precipitation. But if this is the case, it might be more efficient to look for our chronology in these glacial ice (or possibly permafrost) cores rather than through tree rings. This possibility will be discussed more in depth later.

Despite these difficulties, techniques have been developed at the Laboratory of Tree-Ring Research at the University of Arizona (Stockton, 1971; Stockton and

¹An exception might be trees growing along rivers (an example of which will be given).

Fritts, 1971) for reconstructing hydrologic records from tree-ring data. Multivariate analyses are used to correlate tree-ring widths with the existing measured runoff series and then these relationships are used to hindcast the runoff record using the tree-ring record. In the region of our interest here, Stockton and Fritts (1973) have used relatively old white spruce trees growing along natural levees in the delta region of Lake Athabasca to reconstruct a 158-year time series of lake levels (see Stockton and Fritts (1973) for details). In figure 6 we show the location of the trees used in this reconstruction, in figure 7 we show the tree series, and in figure 8 we show the reconstruction of lake levels. The authors note that prior to 1800 the confidence in these series is low due to a smaller number of available trees.

We see in figure 7 that in this century the period 1920-1940 was a period of above-average growth for the delta trees with 1935 being exceptionally high and 1927 low. The period 1955-1976 was a period of above-average growing conditions for trees on the delta region. Preceding this period of high growth was an 18-yr period of low growth (1938-1955). It is proposed that this period of low growth is perhaps due to below-normal soil moisture. An upward trend in growth is seen between 1966 and 1970.

How do these series compare with the MacKenzie discharge? Unfortunately, the only highly-reliable data for MacKenzie discharge (figure 2) does not overlap these tree ring series. The longer time series for discharge off North America into the Arctic (figure 4), as we mentioned, is compiled from many discontinuous observations, covers a much larger runoff area than just that of the MacKenzie, and hence is probably not a highly accurate indicator of MacKenzie discharge. Nonetheless, we see that the North American runoff was high in the mid sixties tandem with increased tree growth. Through the rest of the century there appear to be no strong low-frequency correlations.

By selecting trees closer to the MacKenzie Delta, the potential exists for obtaining a better correlation between tree ring series and runoff. The problems, other than those mentioned, include the fact that as we approach the Arctic, trees become scarce. Furthermore, climate-growth relationships in the North American sub-Arctic are poorly understood (Garfinkel and Brubaker, 1980) and more basic research into these relationships for this area are needed.

2.2 Ice Cores

Now we will discuss the use of ice cores in constructing proxy climate data. In particular, we will concentrate on cores taken in the Canadian Arctic Archipelago.

On these island ice caps, accumulation is generally in the form of snowfall, whereas ablation is by melting and run-off from the ice cap. The important point

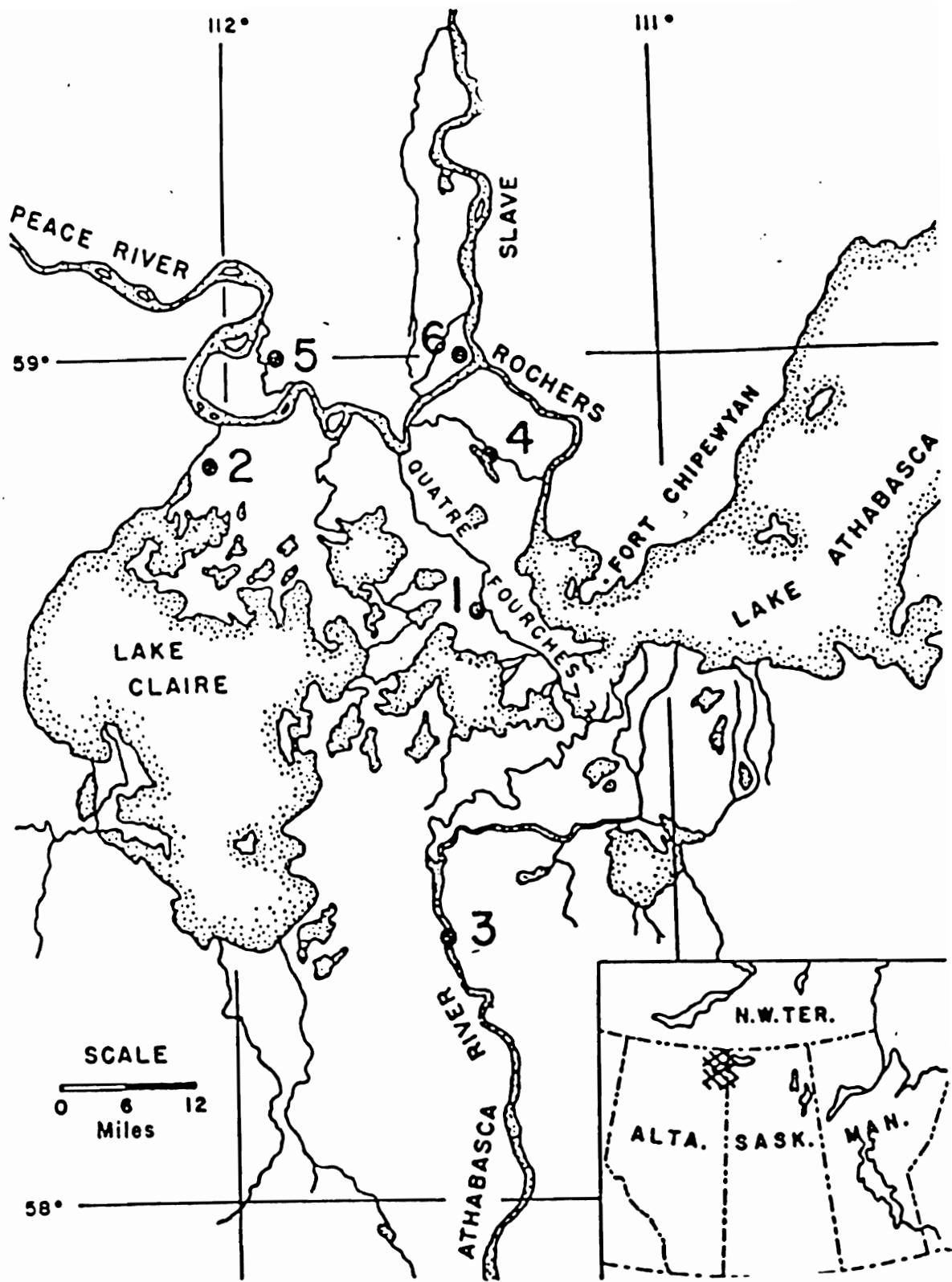


Figure 6: Locations of the 6 tree ring sites. 1: Quatre Fourches; 2: Claire River; 3: Athabasca River; 4: Revillon Coupe; 5: Peace River; 6: Peace River II. Taken from Stockton and Fritz (1973).

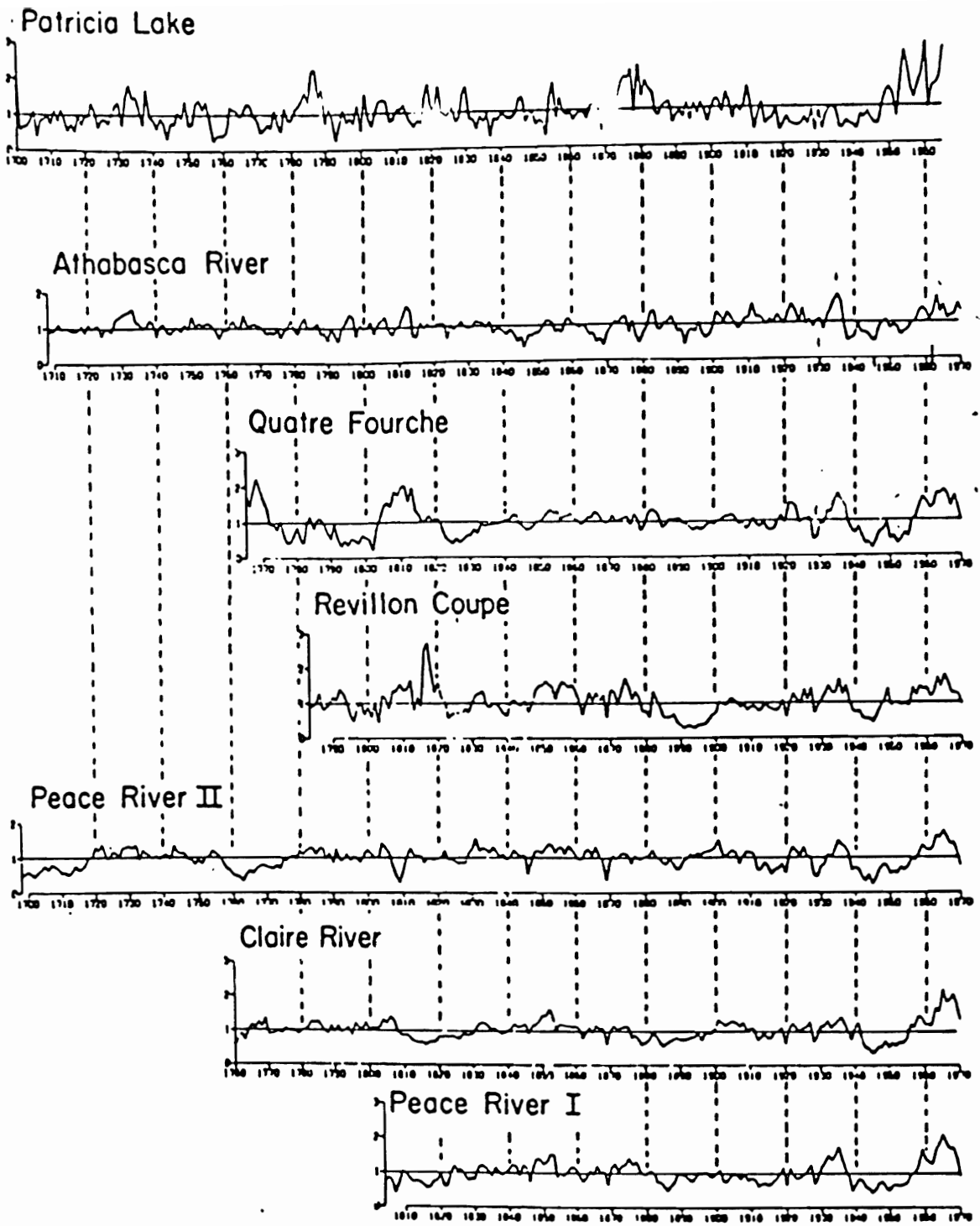


Figure 7: Plots of the individual tree ring series from the Peace-Athabasca Delta are compared with a plot of a tree ring series in the upper Watershed of the Athabasca River (the Patricia Lake series). Taken from Stockton and Fritz (1973).

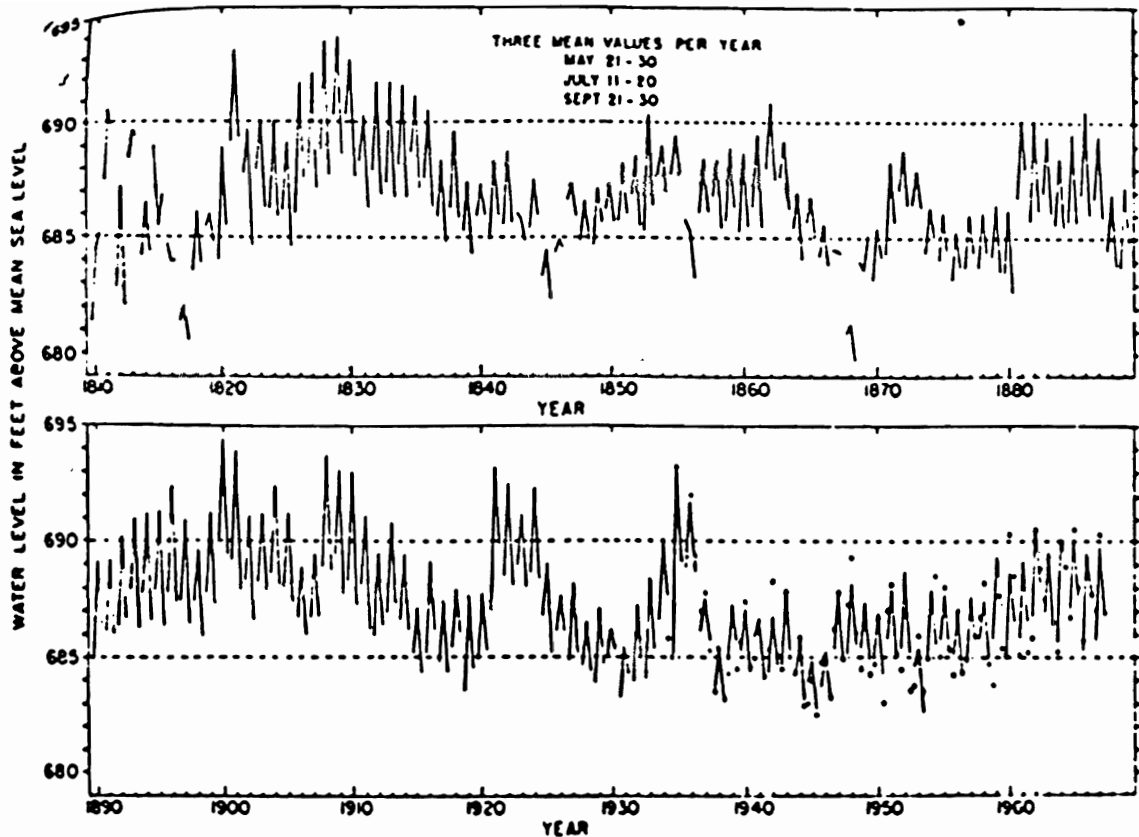


Figure 8: Shown is a reconstructed water level record for Lake Athabasca for the period 1810-1967 (158 years). These values were determined from tree-ring indices of the 6 Delta sites in which both the indices for the year concurrent with and successive to the actual runoff year were utilized as predictors. The actual values for 1935-1967 are also shown, where the circles indicate gauge measurements. The lines join reconstructions for the May, July and September subperiods. (See Stockton and Fritts (1973) for more information.)

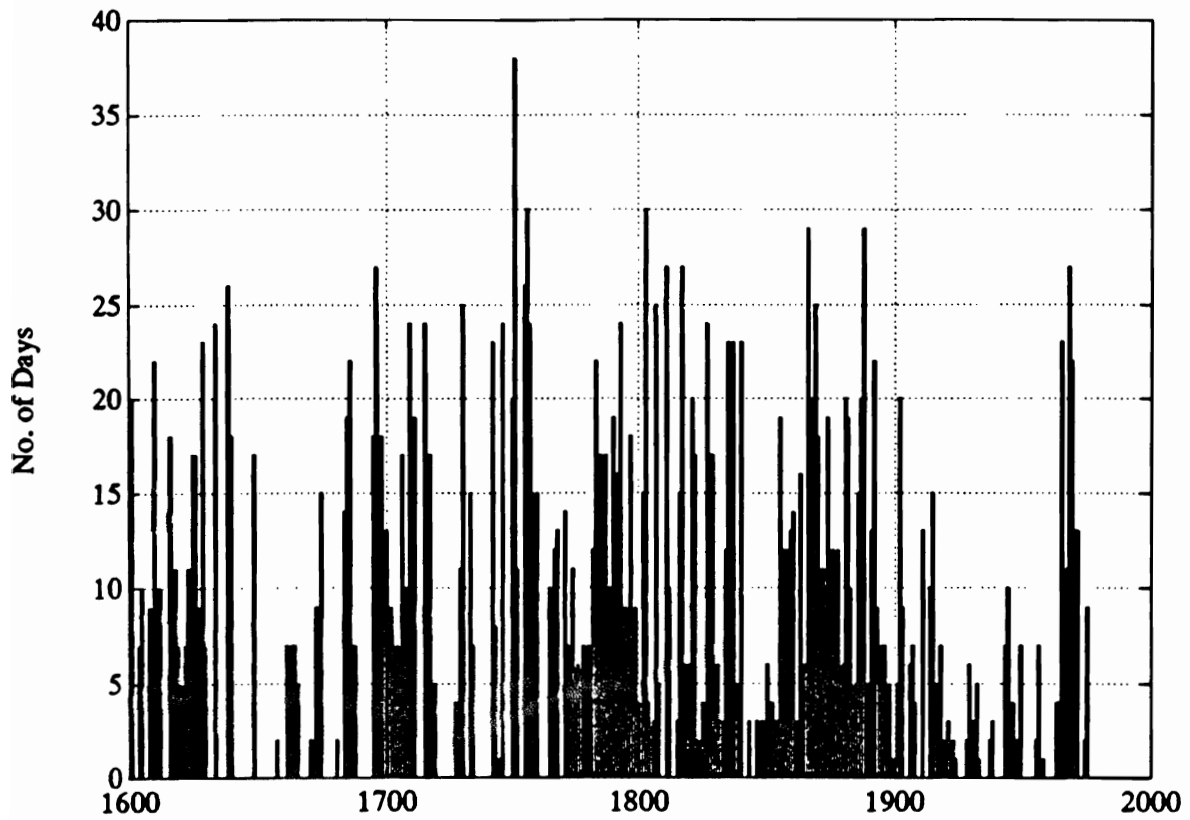


Figure 9: Plotted is the number of weeks per year that ice affected the coast of Iceland (Kelly, 1987).

in ice core studies is that accumulating snow layers traps a variety of aerosols and gases with it. These aerosols and gases remain unchanged for many thousand years (Fisher and Koerner, 1983). Since oxygen exists in two stable isotopes (^{16}O) and (^{18}O), and one (^{18}O) is the heavier of the two, the (^{18}O) concentration in the snow is closely related to the temperature of condensation of that snow. Hence, a (^{18}O) time series can serve as a proxy temperature record (Fisher and Koerner, 1983).

Aside from reconstructing a temperature record from ice cores in the Canadian Archipelago, Fisher and Koerner have also constructed a proxy for summer temperatures using melt features observed in the cores. Briefly, ice that melts in the summer may refreeze within the snow pack either as ice layers or as hard and dense firn. Ice layers from refrozen meltwater can be recognized in ice cores down to a depth of about 150 m—representing about 1,000 years of accumulating snowfall.

These researchers have also successfully related the percentage of ice in each annual layer to both the mass balance of the ice cap and the maximum monthly amount of open water occurring each year in the channels between the Queen Elizabeth Islands (Koerner, 1977). Thus, the authors suggest that melt records may be reviewed (with caution) as proxy summer temperature and proxy sea-ice records (Fisher and Koerner, 1983). However, the annual resolution series exhibits great variation even between nearby core sites (D. Fisher, 1992, personal communication; and as seen in figure 10). Hence, averages over time and space are probably necessary to produce reliable estimates of climate fluctuations.

These ice records offer yearly resolution, extend back several centuries and may to some degree reflect temperatures, melt and runoff. There is a problem in their candidacy for a MacKenzie proxy however. If Mysak and his coworkers are right and sea ice concentration in the Greenland Sea is linked to MacKenzie runoff, then using Canadian Arctic ice cap data as proxy for MacKenzie runoff is equivalent to correlating proxy sea ice concentration from the Canadian Arctic with proxy sea ice concentration from the Greenland Sea (since Koerner and Fisher show that the ice cap data is also proxy for sea ice concentration).

Two other examples of the data taken from these ice cores are shown for ΔO^{18} (proxy for temperature of condensation), shown in figure 11 (a), and ice accumulation (figure 11 (b)).

In as much as the record for ice accumulation on the Agassiz Ice Cap (figure 11 (b)) may be indicative of precipitation (and possibly runoff) over a larger geographic area (as discussed earlier accumulation is generally in the form of snowfall), it is interesting to cross-correlate this precipitation proxy with the Koch ice index (9). The results are shown in figure 12. We see no prominent correlation peaks. Also, the trend for positive correlations (at negative lags) would suggest

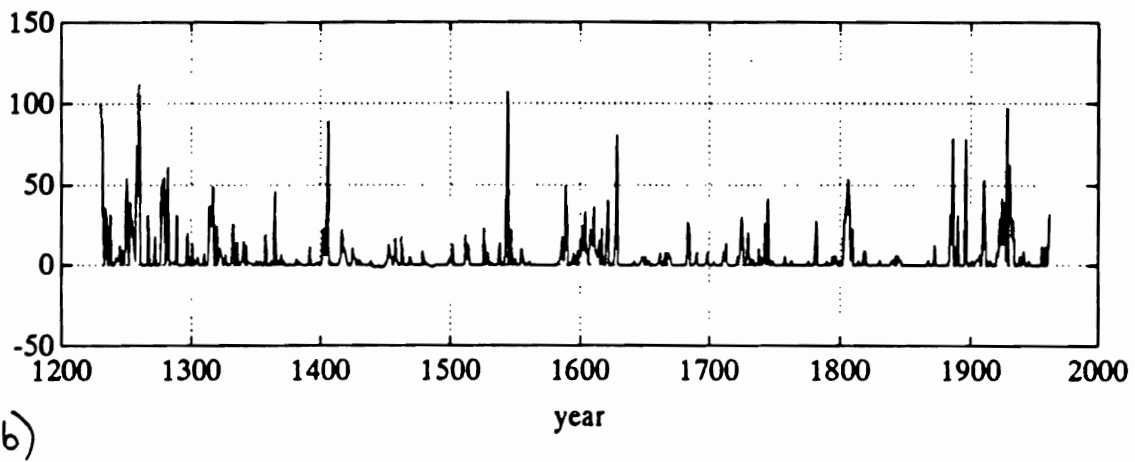
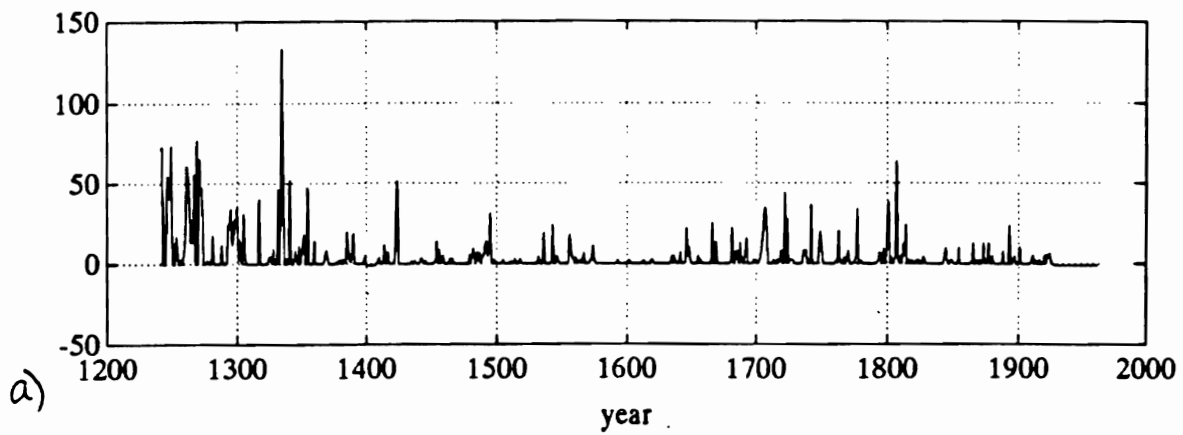
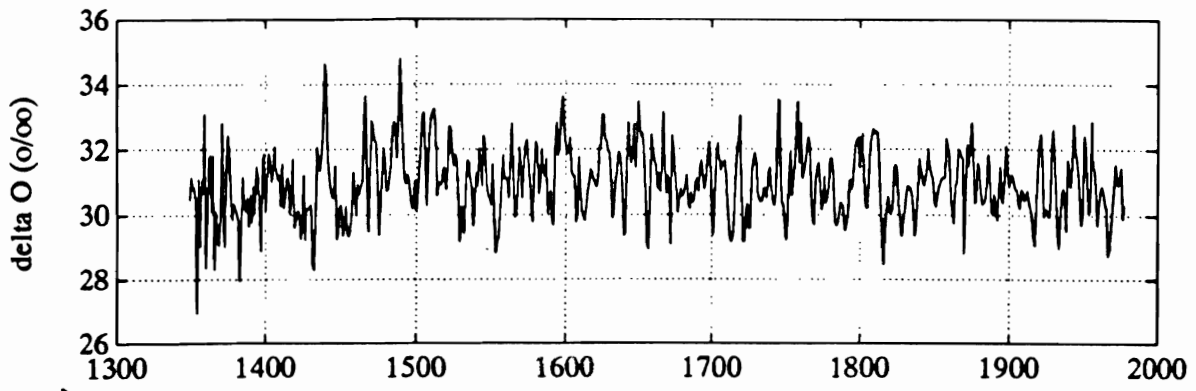
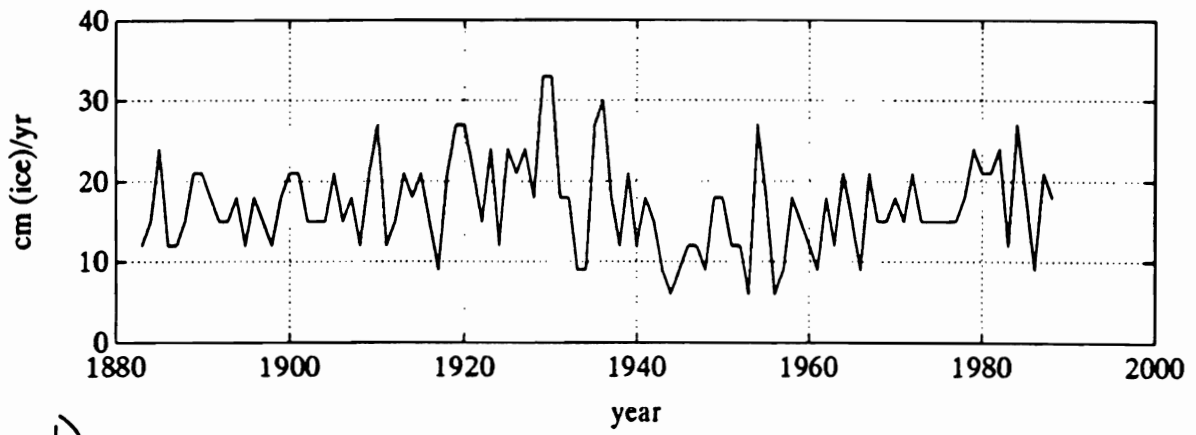


Figure 10: Yearly values of percent ice melt for cores 3-41 (a) and 1-48 (b) from the Agassiz Ice Cap are shown. The volcanic time scale is used and the indexes are such that 100 = all ice, 0 = no ice, and -1 = no data. (See Fisher and Koerner, 1983 for more details.) Data courtesy of D. Fisher.



a)



b)

Figure 11: In (a) we show the ΔO^{18} and in (b) the ice accumulation on the Agassiz Ice Cap (Canadian Arctic). Data courtesy of D. Fisher.

(if anything) that ice off of Iceland leads precipitation in the Canadian Arctic by several decades. For negative correlations (at positive lags), the Koch series lags Agassiz ice accumulation.

A more legitimate approach might be to look at glacial ice cores in the source regions of the MacKenzie. The contribution of glacial melt to the MacKenzie runoff is quite small. However, if the factors affecting glacial melt also affect snow and ice melt over a much larger area of the MacKenzie basin, glacial ice cores may indeed indicate runoff. In a similar sense permafrost records may also be useful. These questions clearly merit a more thorough study.

Before leaving this topic, it is interesting to note that measurements of ice mass balance for glaciers in southern British Columbia (figure 13) bear a resemblance to the existing MacKenzie runoff record (replotted in figure 13) and, as we will see, to magnetic observatory records from nearby Victoria and the southern tip of Alaska (see figures 26 and 25). The resemblance of the ice mass balance and MacKenzie runoff records probably reflect similar large-scale climate processes operating on both. The relationship with the magnetic record will be explored in later sections.

2.3 Sediment Record

The MacKenzie River carries a great amount of silt and exhibits a strong seasonal variation due to glacial melt in the spring and summer. During these seasons, the composition (i.e. grain sizes etc.) will vary and hence we might expect that the seasonal deposition of silt would indicate runoff magnitude and a core through sediment layers in the delta and on the continental shelf would reveal a history of runoff. The problem is that the delta and even the shelf waters are very shallow (≈ 50 m) and storms are frequent. The result is that sediment deposited in these areas are expected to be reworked and the resolution of the sediment record would be ‘smeared-out’ (Fissel and Melling, 1990; M. Lapointe, 1992, personal communication).

One way around this problem might be to search for cores in small tributaries or lakes that would be calm enough to keep from being reworked but still ‘connected’ enough to the main river such that sediment records would reveal river discharge. An anoxic basin would be all the better since burrowing animals can also rework the varved sediment layers and hence the absence of these creatures would be ideal.

Some lakes or tributaries might be found with a critical sill depth that would allow water to flow in from the river only when the river level is higher than the sill. A sediment record in these lakes and tributaries might then serve as a record of sporadic maximum river levels.

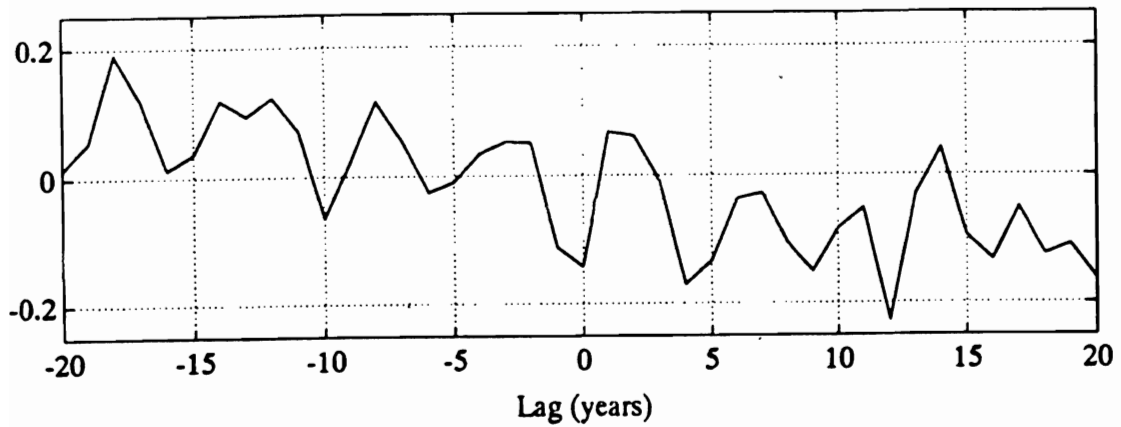


Figure 12: Shown is the lagged cross-correlation function for ice accumulation on the Agassiz Ice Cap (taken as proxy for precipitation) and the Koch ice index off Iceland. (For positive phase, Koch lags ice accumulation.) No strongly significant correlation peaks are observed (95 percent significance levels are located at $\pm .20$) but information might be contained in the observed lag (see text).

GLACIER NET BALANCE VARIATIONS CANADIAN WEST COAST, 1965-90

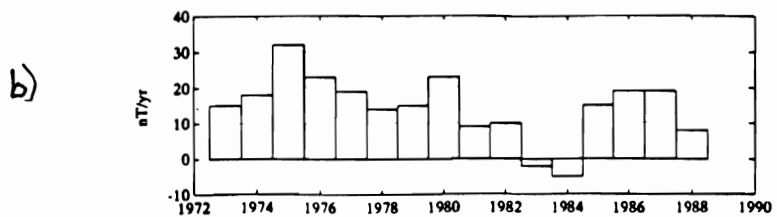
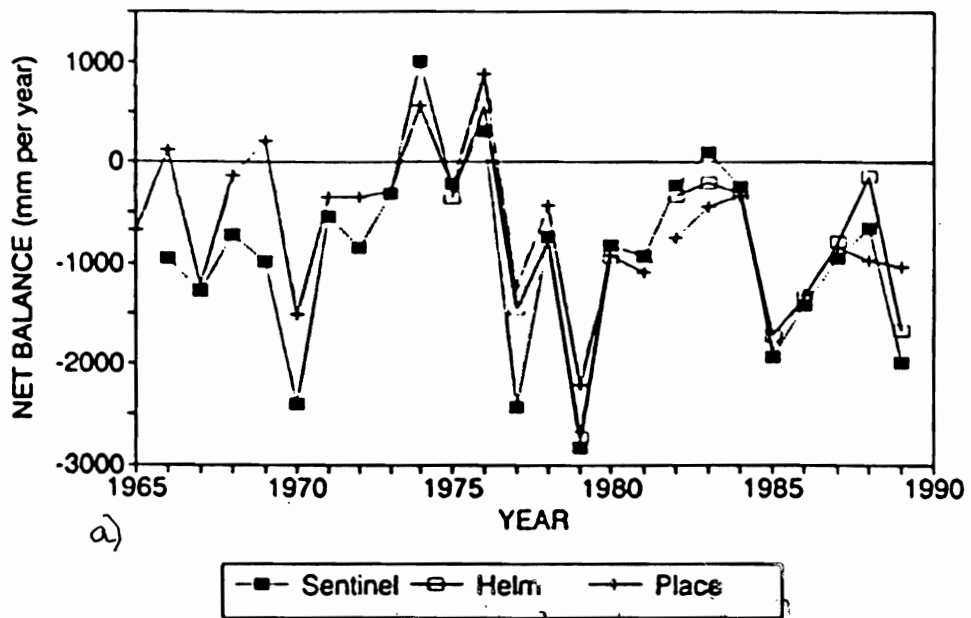


Figure 13: Net Balance of Canadian west coast glaciers (Sentinel, Helm and Place) is shown in (a) (taken from Oestrum and Brugman (1991)). In (b) we have redisplayed the series for the MacKenzie runoff (2).

Another possibility would be to compare the relative concentrations of freshwater and saltwater planktonic species in sediments on the shelf near the MacKenzie Delta. A problem here will again be that of resuspension of sediments. But perhaps the planktonic signal in sediments could be found in deeper water (if it were found that sediment falls out of the water column faster than the plankton do).

2.4 Historical Data Using Content Analysis

Moodie and Catchpole (1975) have performed a rather interesting reconstruction of freeze-up and break-up dates of estuaries on Hudson Bay. They have used the methods of content analysis—common in the social sciences—to extract environmental data from historical documents. Content analysis involves the classification and enumeration of information. In this context, dates are derived from the number of observed occurrences of words related to freeze-up and break-up. The researchers are, however, pragmatic enough to accept a concrete statement when they find one.

We do not expect that this inferred data—even if valid—can help us in our search for a MacKenzie runoff proxy since we do not expect that Hudson Bay runoff and MacKenzie runoff are necessarily similar. We have included this idea here, however, because of its potential use as an indicator of ice severity. (The score is currently 3-nothing; we have three potentially good indicators of ice concentration—the Koch index, Canadian Arctic ice cores, and now this—but so far no easy candidate for the MacKenzie runoff with which we would like to compare.)

Moodie and Catchpole have derived several interesting record categories. We looked at the record at Albany (located at the southwest end of Hudson Bay in Ontario) because of the length of the record and the greater amount of directly-referred dates. In figure 14 we show three of these categories over the full records of each. Category 1 corresponds to the first day (after January 1) that the sea surface was partly frozen. Category 3 corresponds to the first day the surface was completely frozen, and category 5 is the first day the surface was ice free. We have taken the category 5 record (ice break-up), added 365 days, then subtracted the category 3 record to get an estimate of the length of the winter for that year. This is also shown in figure 14 together with the Koch ice index over a similar time frame.

Next we investigate possible correlations between this long Albany winter-length record we have derived and the overlapping Koch index and Agassiz ice core data.

In figure 15 (a) we show the lagged cross-correlation function for the Albany

winter length and ΔO^{18} record (taken as indicative of annual temperatures at Agassiz). As we see, only one barely significant positive correlation appears with Agassiz leading Albany by about 3 years.

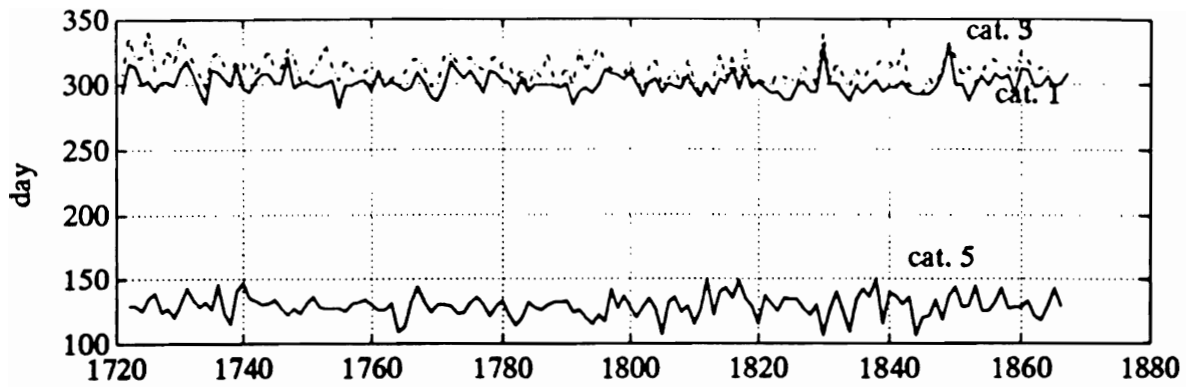
In figure 15 (b) we have the cross-correlation function for the Albany winter length and Koch ice index. Again, no strong correlation peaks occur and, in this case, no consistent lag is observed.

The lack of a good correlation should be expected since the Hudson Bay estuaries probably do not reflect large-scale ice anomalies, and also—in as much as discharge is directly important—the discharge on Hudson Bay reflects a different runoff regime than that of the MacKenzie, as we mentioned earlier. Still, and particularly because the Hudson Bay is protected from deeper ocean dynamics, this reconstruction may be useful as a control set. If ice anomalies in the Greenland Sea and runoff/ice anomalies in the Beaufort Sea prove to be correlated with each other but not with the Hudson Bay (and if Moodie and Catchpole’s reconstructions reflect something greater than local estuarine processes) then there is support of the idea that these anomalies in the Beaufort are advected across the Arctic to the Greenland and Iceland Seas. But if these anomalies are part of an interdecadal cycle that involves precipitation over North America it is not evident that they should be unrelated to Hudson Bay winter-lengths. Here, we may not have given the Hudson Bay records appropriate attention.

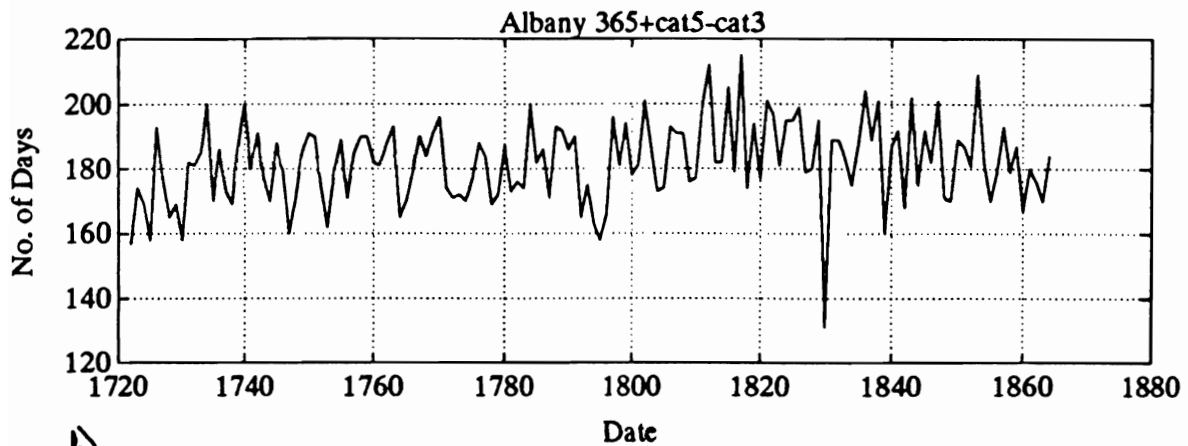
In our search for proxy runoff data we have reviewed above some of the conventional high-resolution proxy sources for climate records. Now we will explore our proposition that geomagnetic observations may be used as proxy for MacKenzie runoff.

3 Motionally-Induced Electromagnetic Fields in the Sea (MIEFS)

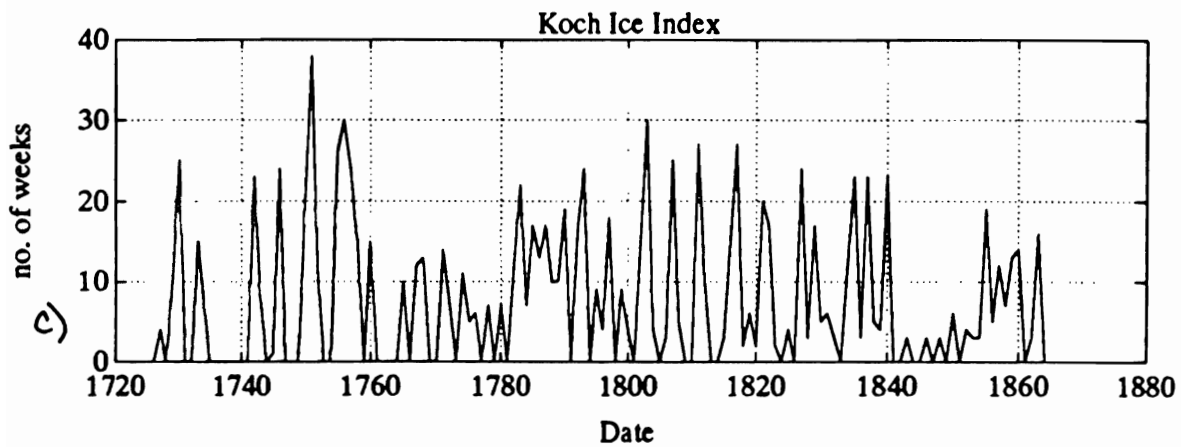
In this section we will describe how the ocean currents flowing through the Earth’s magnetic field can induce secondary magnetic fields that are measurable at distant land locations. We show that data from permanent magnetic observatories in the Canadian Arctic are well correlated with MacKenzie river runoff. We also show that the annual cycle of transport through the Bering Strait appears to be evident in geomagnetic observations at Barrows, Alaska. These correlations, we believe, are due to the fact that the conductivity of the ocean increases with salinity. Hence, magnetic fields produced by the ocean currents moving across



a)



b)



c)

Figure 14: In (a) we present the historical record at Albany, Ontario for categories 1, 3, and 5, as described in the text. In (b) we have an estimate of the winter length (as described in the text), and in (c) we present the Koch ice severity index for a similar span of time.

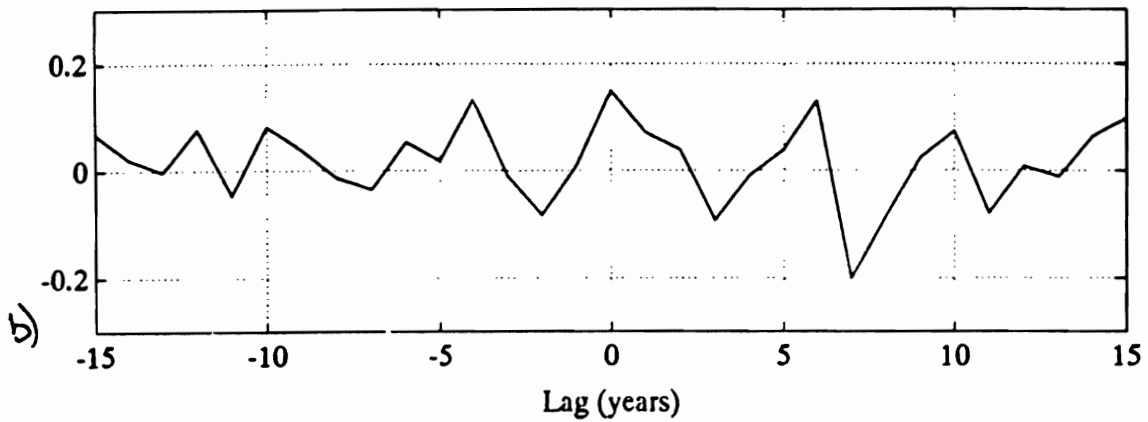
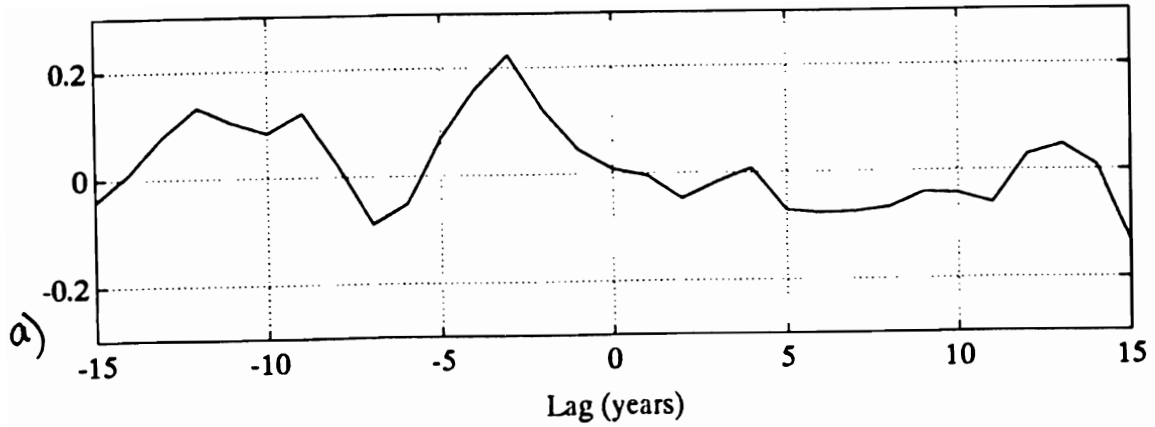


Figure 15: In (a) we show the lagged cross-correlation function for Albany winter lengths (as derived in the text) and ΔO^{18} from the Agassiz Ice Cap in the Canadian Arctic. In (b) we have the lagged cross-correlation function for the Albany winter lengths and the Koch ice index. Positive lags indicate ΔO^{18} (or Koch) lagging the Albany record. The 95 percent significance levels are at about $\pm .18$ on each of these diagrams. (See text for more discussion.)

the earth’s magnetic field (and that depend on the conductivity of the water) will vary with changes in salinity (that may reflect changes in river runoff). Finally, we discuss other ways in which the vast archive of geomagnetic data may be extremely valuable in oceanographic and climatic studies. It is perhaps fortuitous that the potential for extracting oceanographic data from the geomagnetic record is greatest in exactly the regions where conventional data collection has been difficult and historically scarce—the polar regions.

3.1 Theoretical Considerations

What we call ‘salt’ in the ocean is largely a solute of disassociated ions—(Na^+) and (Cl^-) to give examples. As these ions are advected by ocean currents (with velocity \vec{V}) through the Earth’s magnetic field \vec{B} they will be subject to a force per unit charge

$$\vec{F}/q = \vec{E}_m = \vec{V} \times \vec{B} \quad (1)$$

as a consequence of Faraday’s law of induction. This force will tend to separate charges and produce an electric field \vec{E}_m perpendicular to the ocean flow that can in turn produce electric currents that induce a secondary magnetic field. The physics behind this process is more fully explained in Longuet-Higgins et al. (1954) and Sanford (1971).

For illustration consider the case of a current with rectangular cross-section moving through an other-wise still fluid (figure 16). The current V is in the positive y direction and a uniform magnetic field acts in the negative z direction (downwards). By equation 1 we expect that within the current, a force will act to draw positively-charged ions toward the left (negative x) and negatively-charged ions toward the right (positive x). In a frame of reference moving with the current, we can define an electromotive force \mathcal{E}_m by integrating (1) over a closed loop C in the $x - y$ plane (see figure 16)

$$\mathcal{E}_m = \oint_C \vec{E}_m \cdot d\vec{s} = \oint_C (\vec{V} \times \vec{B}) \cdot d\vec{s}. \quad (2)$$

which for this geometry reduces to

$$\mathcal{E}_m = \int_0^L -VBdx \quad (3)$$

If we take as our loop of integration C a line shown as the dotted line in figure 16 equation 3 gives

$$\mathcal{E}_m = -VBL. \quad (4)$$

Hence, positive charge may be driven in the negative x direction within the fluid current while the return charge is carried by the surrounding motionless fluid.

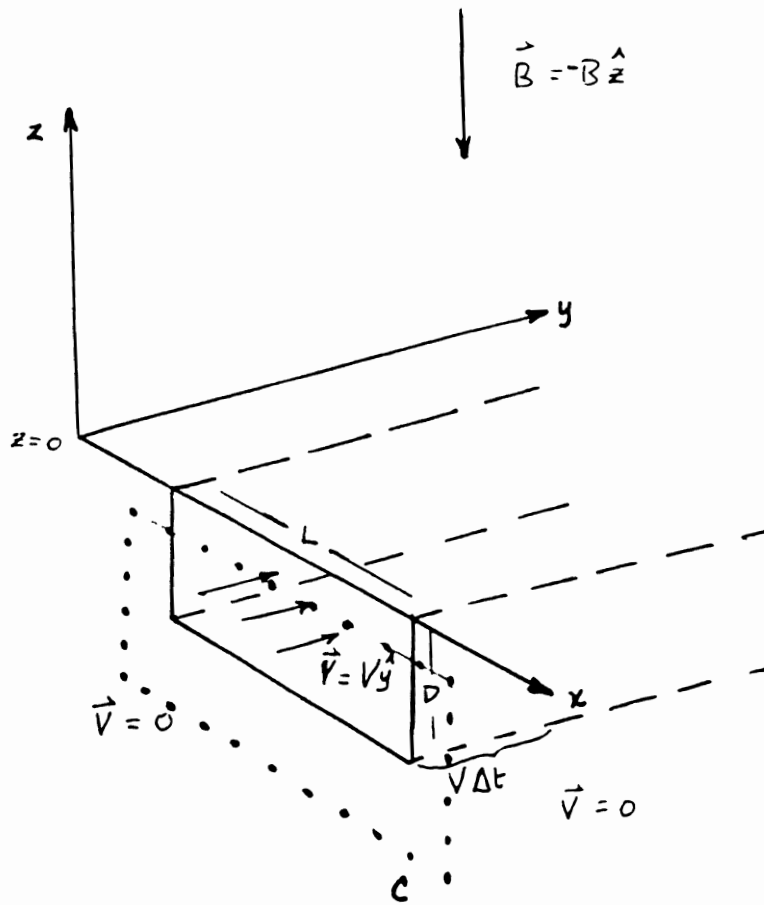


Figure 16: Illustration for description in the text of motional-induced electromagnetic fields in the sea (MIEFS).

This is somewhat reminiscent of an LR circuit, with the fluid motion acting as the battery (or seat of electromotive force \mathcal{E}_m), a resistance R within the return electrical flow, and possibly an impedance due to magnetic fields produced by the electrical loop. The effect of the impedance on the electrical current will be transitory and the steady balance will simply be

$$\mathcal{E}_m = IR \quad (5)$$

where I is an analogous total electrical current, and R the total resistivity. To transfer from this macroscopic analogy back to our problem (which should involve current densities \vec{J} and resistivity ρ (or its inverse, conductivity σ) we note that \vec{J} is simply

$$\vec{J} = \vec{I}/A \quad (6)$$

where A is the cross section through which the current flows (in this case $A = (v\Delta t)D$). Also, it can be show (see for example Wangsness, 1986) that R and σ are related through

$$R = \frac{L}{\sigma A}. \quad (7)$$

Using equations 4, 5 and 7 in 6, we see that we can write the induced electrical current through the moving fluid as

$$J = -\sigma VB, \quad (8)$$

where the negative sign indicates that the electrical currents for the geometry in figure 16 will flow in the counter- clockwise sense.

The next step is to show that these electrical currents flowing in a plane perpendicular to the fluid current V will induce a magnetic field in line with V .

Consider again the closed circuit denoted by the dotted line in figure 16. Along this circuit we can expect a current flow in the counter clockwise sense. It is well known that an electrical current along a closed loop will induce a magnetic flow through this loop. In the case of the loop here, the induced magnetic field would act in the negative y direction. We can gain an estimate of this induced field using Maxwell's equation for the curl of the magnetic field for a steady field while we neglect the flow of current arising from sources other than conductivity:²

$$\nabla \times \vec{B} = \mu\sigma\vec{E}, \quad (9)$$

which for this geometry can be approximated as

$$\Delta B \approx \mu\sigma E\Delta z = \mu\sigma VB\Delta z. \quad (10)$$

²Advection of ions by fluid transport is here considered to be small relative to conduction current velocities.

Here, μ is the magnetic permeability, taken everywhere equal to $4\pi \times 10^{-7}$ (henries/meter). Using the current depth D as an estimate for Δz we see that ratio of the induced magnetic field ΔB to the background magnetic field B (representing here the geomagnetic field) will be of order

$$\frac{\Delta B}{B} \approx \mu\sigma VD. \quad (11)$$

In the case of the Earth, the vertical component of the magnetic field is the largest in the polar regions (we will see below that because of the aspect ratios, this is the most important component). Hence, by equation 11 we note that the induced magnetic fields may be especially large in the polar regions. There are other reasons why induced electromagnetic fluctuations may be particularly salient in the polar regions but before we discuss this we will take a moment to review the theory of motionally induced electromagnetic fields in the sea (MIEFS) including a bit more rigor. In particular, we have not yet discussed the importance of conductivity variations, the dielectric influences and how fluid shear geometries other than the one presented here may not have as readily available a path for the return electrical current flow.

The conductivity of seawater is generally much greater than that of the sea bottom. Also, air in this context is essentially an insulator ($\sigma \approx 0$). As we have seen, the induced magnetic field will generally depend on conductivity. For the case that we have been considering with a fluid current surrounded by stationary fluid, we can view the return electrical current as returning through ocean water at rest and neglect current flow through the ocean bottom.³

The conductivity of seawater depends principally on three factors—pressure, salinity and temperature. The effect of pressure on conductivity is only about 5 percent over the whole ocean depth (about 5 km). Also, since salinity in the World’s ocean is surprisingly uniform, Filloux (1987) has argued that conductivity is essentially a function of water temperature (see figure 17). The case in the Arctic, however, is quite different. Here we have almost the contrary case where temperature is quite uniform and because of ice formation/melt and the large river flux into the Arctic, salinity variations are large. Hence in the Arctic, we argue, conductivity will mainly be a function of salinity. We show this by presenting a contour plot (figure 18) showing the variations of conductivity due to the range of salinity and temperatures found in the Arctic surface waters. Conductivity is clearly dominated by variations in salinity in this region.

We have so far not included the dielectric effects that must be present due to the electric field passing through the electrically polar water molecules. It is

³This probably remains a fair approximation for surface currents in deep water.

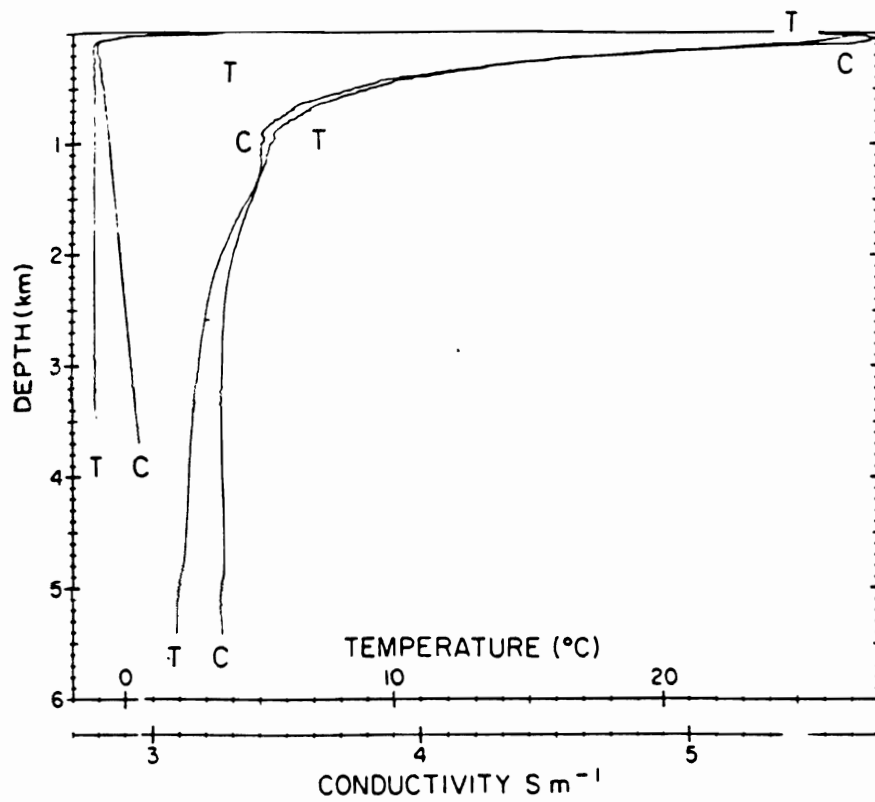


Figure 17: Sea-water temperature and conductivity σ as functions of depth for extreme cases in the North Atlantic. Taken from Filloux (1987).

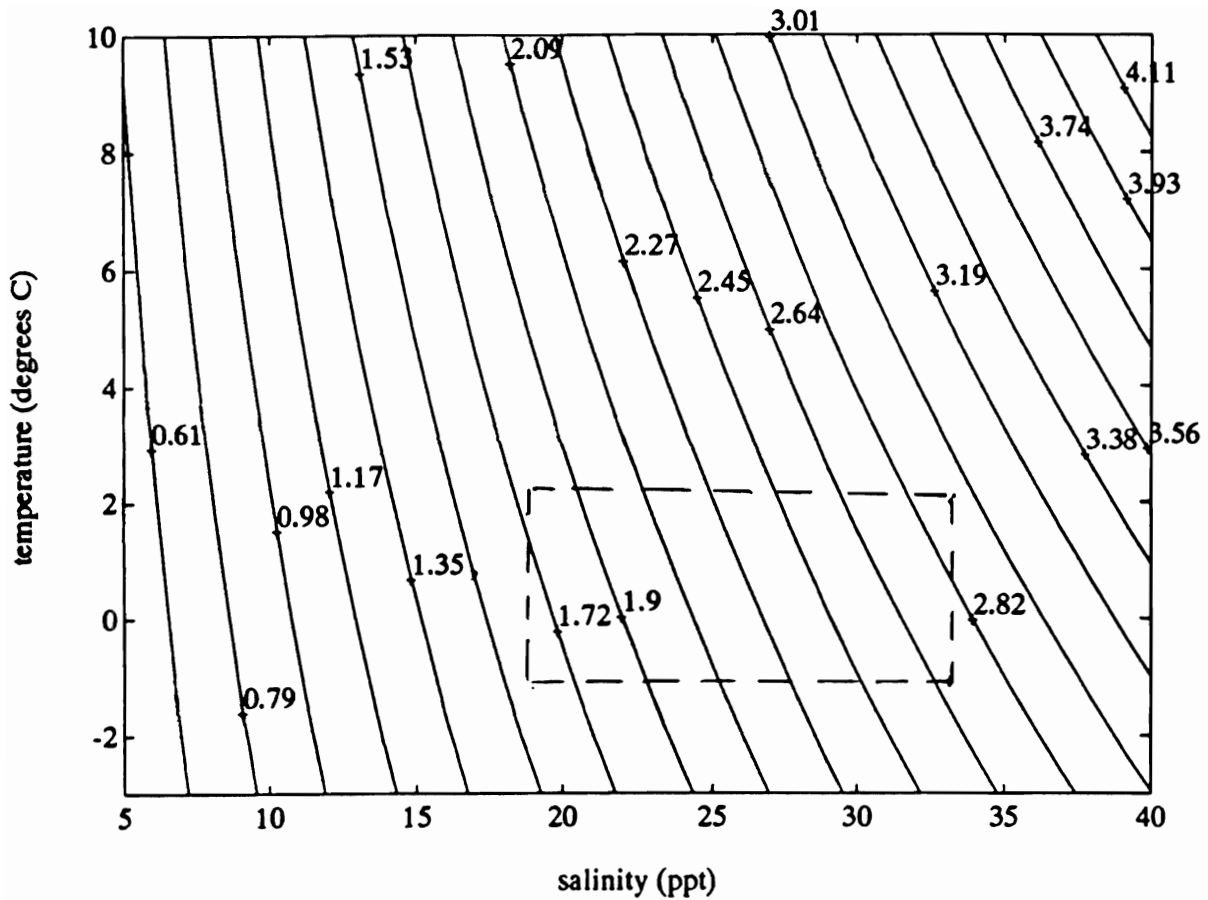


Figure 18: Ocean conductivity σ is shown for the range of salinity and temperature found in Arctic waters. Units are siemens per meter (S/m). Outside of estuaries, most arctic waters probably fall within the dashed box.

easily shown that this effect is much less important than the conduction effects—seawater acts more as a conductor than a dielectric (see Sanford (1971) for an example of this scaling argument).

Now we consider ocean currents passing through a realistic geomagnetic field. First of all, we will consider only ocean surface currents over a deep ocean that are quasi-steady in time. This should approximate much of buoyancy and wind-driven circulation. This creates a great simplification since electrical currents can be taken as passing explicitly through water and the conductivity can be estimated by an average conductivity over the depth in which the electrical induction takes place.

Variations in the earth’s magnetic field \vec{B} will take place over scales much larger than a typical ocean depth, and since ocean currents principally flow in the horizontal plane in the Arctic we can write the equation for the motionally-induced electric field (equation 1) as

$$\vec{E}_m = (V_y \hat{x} - V_x \hat{y}) B_z - V_y B_x \hat{z} \quad (12)$$

where we have used the coordinate system shown in figure 19.

When we consider that the Earth’s magnetic field has the basic form of a magnetic dipole with field lines emanating from the Antarctic region and entering the Arctic region, we see that for low latitudes where B_x is important (and $B_z = 0$) the induced field \vec{E}_m will in general depend on the zonal oceanic flow and acts in the vertical sense. The resulting electric current and induced magnetic fields may be especially complicated. Also, since the induced seat of electromotive force \mathcal{E}_m is essentially scaled with the ocean current depth, and return electrical flow on either side of the ocean currents will tend to induce magnetic fields in opposing directions, the resultant magnetic field measured at a remote location is probably both small and difficult to interpret.

In the polar regions, however, where B_z is the important component⁴ the induced electric field is essentially

$$\vec{E}_m = VF\hat{l} \quad (13)$$

where V is the ocean current magnitude, \hat{l} is a unit vector acting in the horizontal plane and toward the left (right) of the ocean current velocity in the northern (southern) hemisphere, and F is the magnitude of the geomagnetic field strength, taken as $F = 60,000$ nanoTeslas (nT).

The resulting electric currents will induce secondary magnetic fields. We are interested in estimating the direction and magnitudes of such magnetic fields

⁴We have been making a comparison of polar and low-latitude regions for illustration. Both components B_z and B_x will be substantial over much of the globe.

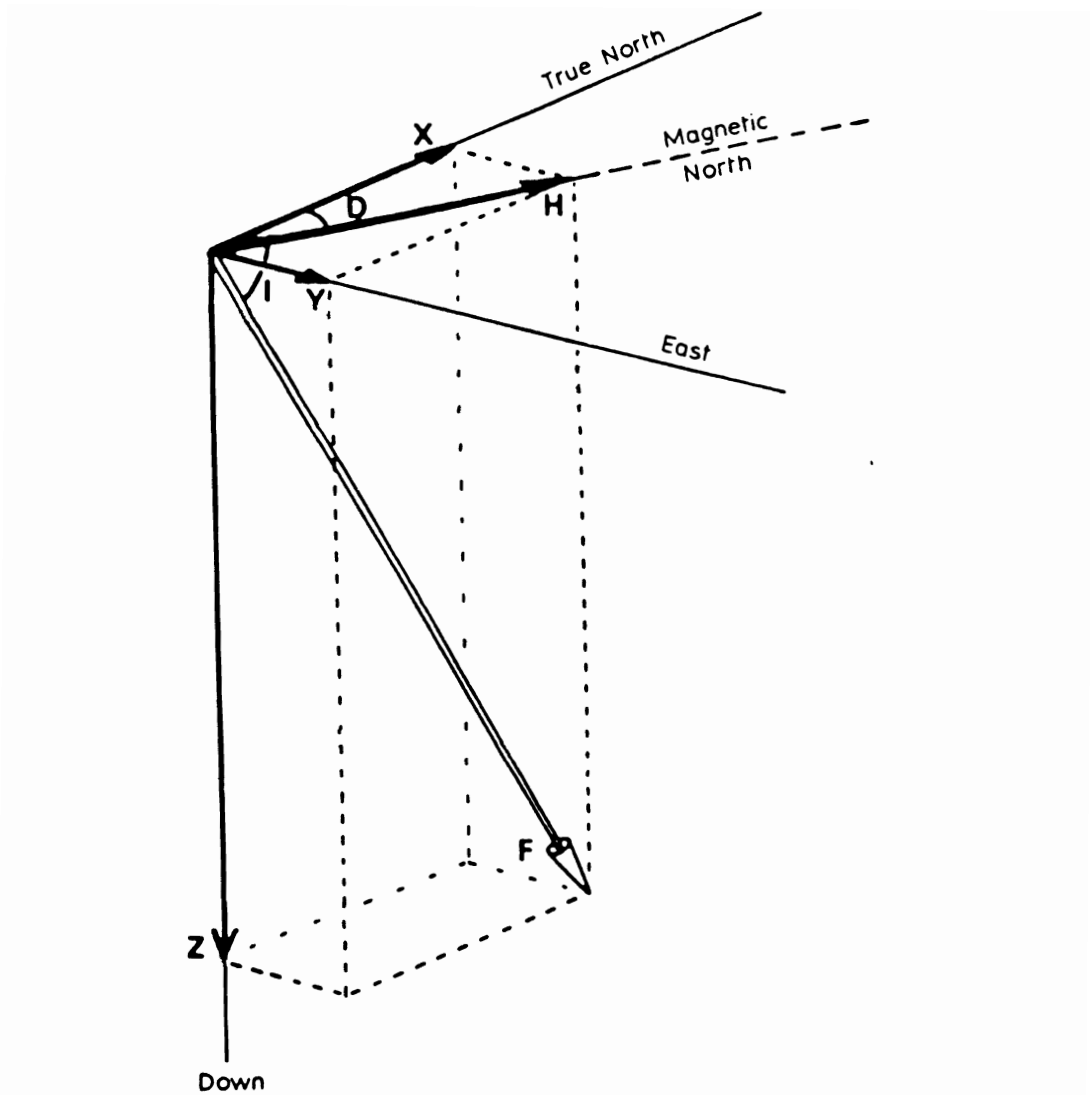


Figure 19: Shown is the coordinate system used in geomagnetic studies. Reference frame and various conventions: x -axis to true North; y -axis to East. D_c is the declination (the angle with true North). Taken from Malin (1987).

measured not within the ocean but at observatories on land nearby. Both the direction and the magnitudes measured will depend on the particular geometry of the ocean current. Nonetheless, we can use limiting cases to gain some insight.

It is easy to show using the integral form of Ampère's Law

$$\oint_C \vec{B} \cdot d\vec{s} = \mu I_{enc}, \quad (14)$$

where the integral is taken about an arbitrary closed path C and I_{enc} is the total current passing through the area *enclosed* by the curve C , that the magnetic field induced by an infinite-plane ocean current is

$$B' = \frac{1}{2}\mu K \quad (15)$$

where μ is the electrical permeability, K is the current per unit length, and an apostrophe is used to distinguish the induced magnetic field from the geomagnetic field. Also, K can be written as the current density multiplied by the thin depth of the current D :

$$K = JD. \quad (16)$$

The direction of the field B' is parallel to that of the ocean current for the region above the ocean current and antiparallel for the region below. Combining equations 15 and 16 we have for the magnetic field magnitude

$$B' = \frac{1}{2}\mu JD. \quad (17)$$

We can use equation 8 in 17 (switching the notation for the geomagnetic magnitude B to F to avoid later confusion) to obtain for the magnitude of B'

$$B' = \frac{1}{2}\mu F(\sigma VD). \quad (18)$$

When we consider as argued earlier that the conductivity in the Arctic is a function essentially of salinity, the term in parenthesis in equation 18 can be thought of as a measure of salt transport. Since F is known, observations of B' might reflect the transport of salinity by ocean currents in the regions.

Ocean currents are not infinite planes as assumed in the previous derivation. Furthermore, observatories are located on land and as such are not positioned either above or below the current planes. Induction by realistic currents could be tackled numerically. Here though, we can make some rough estimates. Currents associated with circulation will usually be of large enough scale that nearby magnetic observatories will record the induced magnetic vectors in a direction roughly

parallel to that of the currents. Exceptions might be for observatories directly in front of or behind large currents. In this case curvature of the earth might predict that these observatories will be ‘looking down a solenoid’. Or, put another way, the magnetic field under the ocean current (which would normally be pointing in the direction opposite to that above the current) may extend ahead and out of the water owing to the Earth’s curvature and what would be measured could be in a direction opposite to that of the ocean currents. Such a coincidence of observatory location and current geometry may well exist with the Alert observatory in the Canadian Archipelago and the facing Transpolar Drift. In this light, it would be interesting to measure the magnetic vertical profile at this location.

We will be discussing observed data shortly. Before doing this we should mention that since realistic ocean currents are not infinite planes, we should also expect that the magnitudes of the induced magnetic fields will drop off with distance away from the source. This effect is difficult to calculate since it is sensitive to the realistic current and location. However, with what is known of induction around other geometries (such as infinite current filaments and dipole loops) we suggest here that the magnetic variations due to ocean currents probably drop off as $L(\frac{r_o}{r})^\alpha$ where L is a typical length scale of the current, r_o is a reference distance, r is the distance to the observatory and α probably has a value in the range

$$1 < \alpha < 3. \tag{19}$$

This field dependence will become important if we consider observations at distances r much greater than the scale of the inducting currents L .

We can then summarize by saying that oceanic surface currents may induce parallel magnetic fields $B'(r)$ measured at remote observatories with magnitude

$$B'(r) \approx F(\sigma VD)L(\frac{r_o}{r})^\alpha \quad 1 < \alpha < 3. \tag{20}$$

In the next section we will examine geomagnetic data from permanent observatories in the Arctic and show that the observations indeed seem to indicate the presence of induced fields as described. Furthermore, we will show that the MacKenzie runoff appears to be correlated with magnetic observations in the Canadian Arctic and on the Pacific Coast of Canada and Alaska.

3.2 Magnetic Observations

In figure 20 we show the locations of the magnetic observatories in the Arctic region. To test the ocean salt-transport/magnetic relationships we have discussed, we will start by discussing data taken from Cambridge Bay (CBB) and Resolute Bay (RES) in the Canadian Arctic Archipelago. We show that measurements

taken here appear to reflect the discharge from the MacKenzie. Then we compare magnetic data from Barrows Alaska (BRW) with estimates of monthly transports through the Bering Strait. Finally, we will discuss wider applications of these methods.

We see from (figure 20) that Cambridge Bay is located in the path of MacKenzie runoff (some of the buoyancy- driven circulation is expected to flow from the Beaufort to the Labrador Seas via the Archipelago). We also note from this map that the drainage and contact with the open ocean is restricted. The station at Resolute Bay, we expect, is also in the path of MacKenzie runoff. However, the contact with the open ocean may be more important at Resolute than at Cambridge Bay.

To make an estimate of the magnitude of MIEFS we will need to estimate the salt transport in this region. We argue that because of the restricted flow, over short time scales the situation near Cambridge Bay is roughly represented by imagining the MacKenzie as a freshwater addition to a solute basin with an otherwise sluggish inflow and outflow. Then, the rate of change of salinity is proportional to the rate of change of volume. That is, the rate of change of salt transport should be correlated negatively with MacKenzie discharge (which is a measure of the rate of freshwater addition). Since by equation 18 we expect magnetic variations to be proportional to salt transport, we expect here, for the case of Cambridge Bay, to see a negative correlation between MacKenzie runoff and the time rate of change of magnetic strength variations due to MIEFS. In figure 21 (a) we indeed see a strong correlation between the rate of change of the magnetic field in the horizontal plane \dot{H} and the MacKenzie runoff (seen in figure 21 (b)) but the sign of the correlation is positive rather than negative.⁵

In constructing our theoretical ideas in the last section, only idealized geometries were considered. If we look at the location of the Cambridge Bay observatory (shown in figure 20), we notice that the observatory appears to be in the path of the westerly-channel flow (and hence, ‘looking down’ the induced magnetic solenoid), while above and west of the flow out the eastern section. Also, other larger channels nearby may be important even if further away from the observatory since we have seen that the distance of influence of these induction currents are essentially scaled by the width of the oceanic flow (which can be taken as the width of the channel).

With these considerations, it is certainly possible that the induced vector fields from these different sources add to give a net result that is positively (rather than negatively) correlated with runoff. Put another way, even if the magnetic fields at each of these channel segments are negatively correlated in magnitude with

⁵We resort to H here when referring to observations to follow historical convention. H should be regarded as representing the B' we used in the calculations.

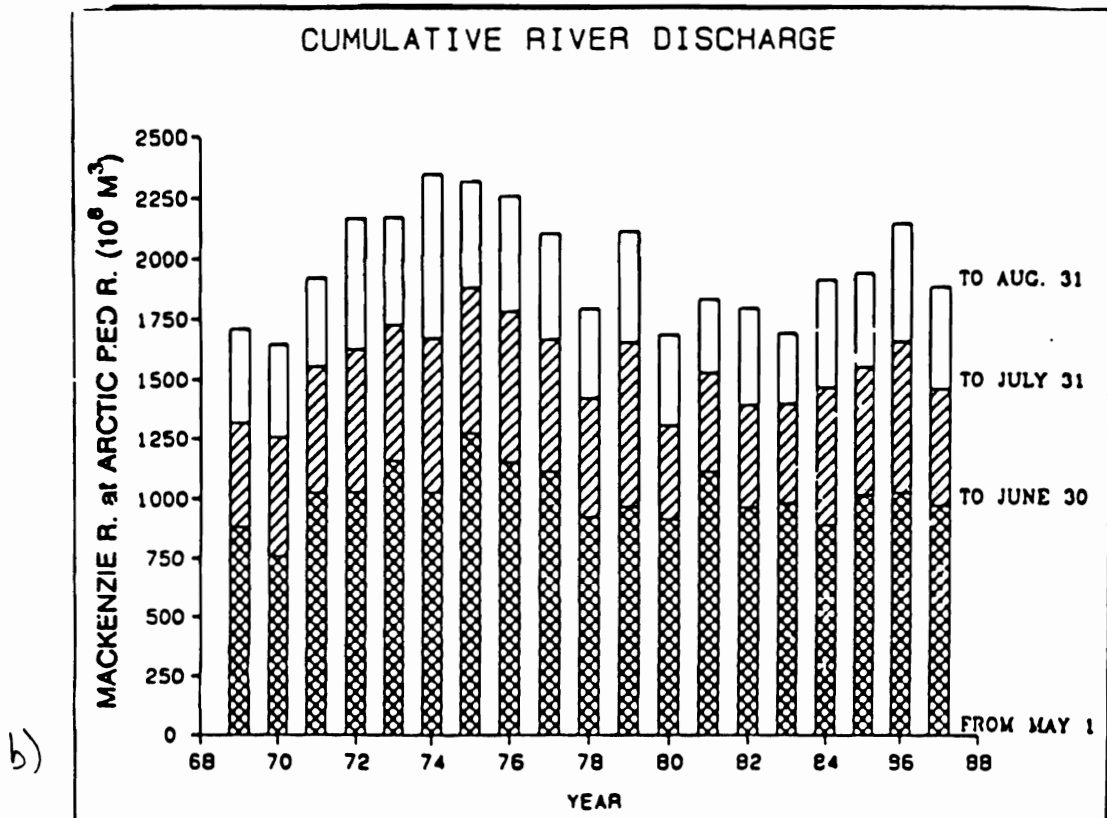
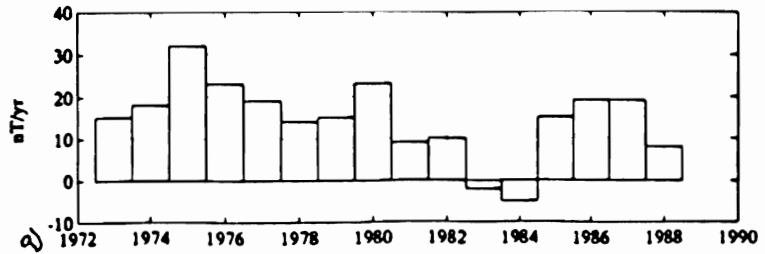


Figure 21: In (a) the changes per year in horizontal magnetic intensity \dot{H} are shown for Cambridge Bay (CBB). In (b) the MacKenzie runoff is replotted for comparison.

runoff, at the location of the observatory, the net ‘vector-addition’ sum of all these components can have a cross-correlation with runoff of either sign.

The positive cross-correlation between the Cambridge Bay \dot{H} observations and MacKenzie runoff may also be explained in another way. Salt transport (effecting magnetic induction) depends not only on salinity variations but also on variations in mass transport. Although increases in runoff decrease the local water conductivity, these runoff increases can also increase the amount of buoyancy-driven transport and at Cambridge Bay the effect of the latter may be more important in producing MIEFS. This is a plausible explanation since we will see next that at Resolute Bay—where buoyancy forcing by the MacKenzie is probably not as important as the background cross-Archipelago gradients—the correlation between MacKenzie runoff and magnetic induction is negative, as we were expecting.

In figure 22 we compare the Resolute measurements of magnetic intensity H with runoff from North America. Here ocean flow is less restricted than at Cambridge Bay and the influence of larger scale ocean dynamics may be more important. We show H with a 10-yr mean removed in (a) and in (b) we present for comparison the MacKenzie and North American runoff series described in figures 2 and 4 with their means removed and with each series divided by its standard deviation. Both segments of the records (taken to represent MacKenzie runoff) shown in figure 22 (b) appear to be correlated with the Resolute magnetic record 22 (a). A better correlation appears in the latter segment, however.

We should estimate the associated magnitudes involved to see if they are consistent with the CBB and RES observations. Since we have argued that changes in magnetic inductance (by MIEFS) at CBB are due to changes in salinity (hence conductivity) and also changes in fluid transport, we can estimate the relative magnitudes of salinity and transport changes needed to bring about the observed changes in inductance.

First, for salinity (conductivity) changes, σ and H are proportional and this relationship can be stated as

$$\frac{\Delta H}{H} \approx \frac{\Delta \sigma}{\sigma} \quad (21)$$

which after considering equation 18 (and remembering we are now using H instead of B') can be put as

$$\Delta \sigma \approx \frac{\Delta H}{\mu F V D}. \quad (22)$$

If we insert rough value estimates in 22 of $F = 60,000nT$, $V = 1m/s$, $D = 50m$, and observe from figure 21 that typical annual variations in H are of order $5nT$, we can estimate $\Delta \sigma$ as

$$\Delta \sigma \approx 1 (S/m). \quad (23)$$

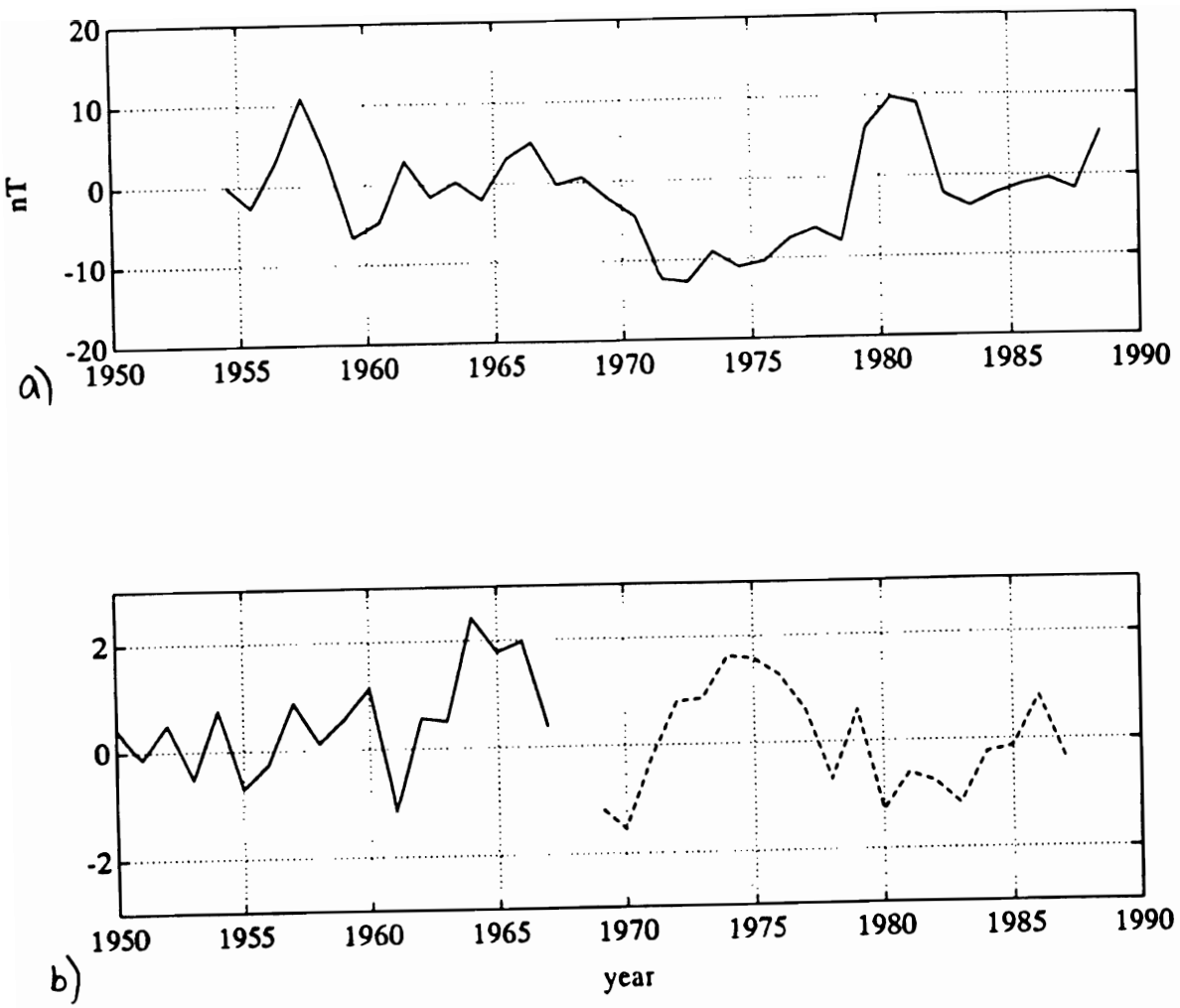


Figure 22: In (a) we show the magnetic intensity in the horizontal plane H measured at Resolute Bay in the Canadian Arctic. A ten-year moving average has been subtracted from the original series. In (b) we display a composite of the runoff records described in figures 2 and 4. Here, the means have been removed and each runoff series has been divided by its standard deviation for display purposes. A cross correlation of these records for the years 1969-1988 shows a 95 percent significant zero-lag with a coefficient of $-.73$ (95 percent = $\pm .45$)

From figure 18 we see that this corresponds to a change in surface salinity of order 10 *ppt*. This is certainly in reasonable agreement with observations.

A similar procedure can be followed for estimating the changes in transport (or the depth-integrated velocity V) that would be needed to account for the observed changes in H . After doing this, we find that the changes in V should be of the order of a few centimeters per second. This also agrees with what we might expect for typical buoyancy-driven current fluctuations in the ocean.

An estimate has been made for the monthly transport through the Bering Strait over the annual cycle (Coachman and Aagaard, 1988). A permanent magnetic Observatory has been in operation in Barrows Alaska since 1933. What we will do now is compare the averaged monthly signal of transport through the strait with averaged magnetic observations at Barrows. Through the strait we will assume that the salinity does not vary much and that it is rather the volume transport that will control inductions in MIEFS variations. (This is probably a good assumption if simply because of the great monthly variation in transport.) The geomagnetic H_g will be pointing roughly northward regardless of MIEFS. An H' due to MIEFS would also act roughly northward. So in this case H' would reinforce H_g and we would expect fluctuations in the total field H would be positively correlated with fluctuations in transport.⁶ Figure 23 shows this monthly Bering Strait transport and figure 24 shows the magnetic field strength H observed at Barrows Alaska.

The correlation of H and transport over the annual cycle is remarkable. Also, the declination variations are again consistent with what we would expect for a magnetic vector that relaxes with decreasing transport in the Winter to a direction closer to that of the magnetic pole (see figure 20 for a location of this pole).

We have seen that the qualitative nature is what we expect. How about the magnitudes? Do the variations in transport account for the variations in H observed? We see from figure 23 that the total transport varies seasonally by about $.5 Sv = 5 \times 10^5 m^3/s$. The *transport per unit length*—which is the only transport we have been using until meeting this figure for Bering transport from Coachman and Aagaard (1988)—is equal to the total transport divided by L , a typical width of the transport which we will estimate as 100 km. The transport per unit length seasonal variation is then of order $5 m^2/s$ and represents Vd in equation 18. Using as a typical conductivity $\sigma = 2$ we see by equation 18 that the

⁶We must be careful since in some locations where the MIEFS-induced H' is in opposition to the background H_g the effect of MIEFS will be to *decrease* the total observed field strength H . In the previous restricted flow problem working with the time derivative had the added benefit of filtering out the slowly varying H_g .

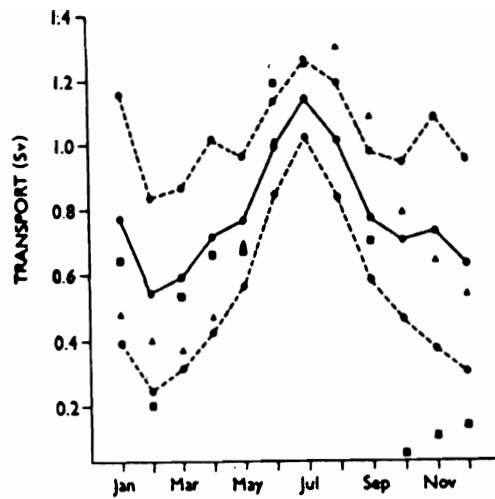


Figure 23: Mean monthly transport through Bering Strait for 1964-1982 (a). Dashed lines denote 1 standard deviation. See Coachman and Aagaard (1988) for more details.

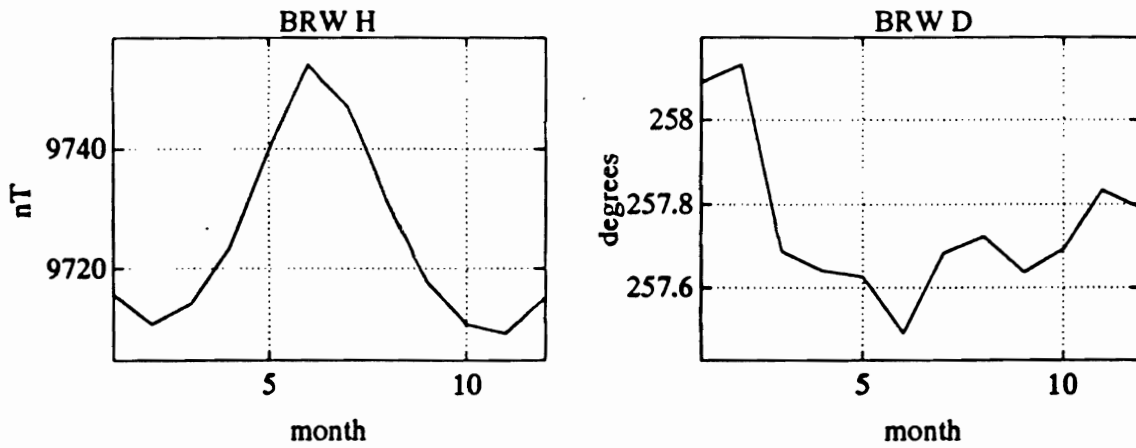


Figure 24: In (a) we show the monthly average magnetic intensity H and in (b) we show the average declination D_c for observations at Barrows, Alaska.

variations in transport would induce a magnetic variation of order 1 nT. We see by figure 24, however, that the observed seasonal fluctuations in H are about 30 times this. It is certainly possible that including a realistic current shear would account for this discrepancy. Also, there is the possibility that a seasonal signal in the Beaufort gyre acts in tandem. The explanation would be plausible if it were found that the Beaufort Gyre has greater vorticity in the summer than winter. Since there seems to be basic controversy over which direction the Gyre rotates (D. Holland, 1992, personal communication) we will postpone discussion related to Beaufort MIEFS:

Earlier we suggested that it was possible that fluctuations in MacKenzie discharge and glacial mass balances in British Columbia were similarly regulated by large-scale climatic factors. This speculation was prompted by observations that magnetic records at Victoria and Sitka (on the North American West Coast) appear to be correlated with the MacKenzie runoff record (see figures 25 and 26).

The cross-correlation coefficient for the Sitka H series and the MacKenzie runoff for the years 1969-1988 reveals a significant positive correlation with Sitka leading the MacKenzie by about a year (the coefficient is .61 and the 95 percent level is at about $\pm.45$). Correlations with Sitka and the earlier runoff series are less obvious.

The cross-correlation coefficient for the Victoria H series and the MacKenzie runoff for the years 1969-1988 shows a significant positive correlation for zero lag (the coefficient is .75 and the 95 percent level is at about $\pm.45$).

Since the MacKenzie does not flow into the Pacific, the most reasonable explanation for the similarities observed would be that large scale climate fluctuations induce melt on both sides of the Rockies and that this melt contributes a dominant signal in both Pacific and Arctic runoff. Such postulations could be verified using records from Pacific rivers. The reader might note that if magnetic records on the Pacific resemble MacKenzie runoff, and magnetic records in the Arctic resemble MacKenzie runoff, then the two magnetic sets also resemble each other and thus may be due to a larger scale solid-earth or ionospheric process. And the resemblance to runoff could be ascribed to one coincidence rather than several. We have investigated magnetic data sets from several other stations and have found this objection to be unsupported.

4 Summary

This report essentially describes a pilot study. In the interest of extending the MacKenzie River runoff record, we have reviewed several conventional proxy sources and the special problems associated with their use for this sparsely-

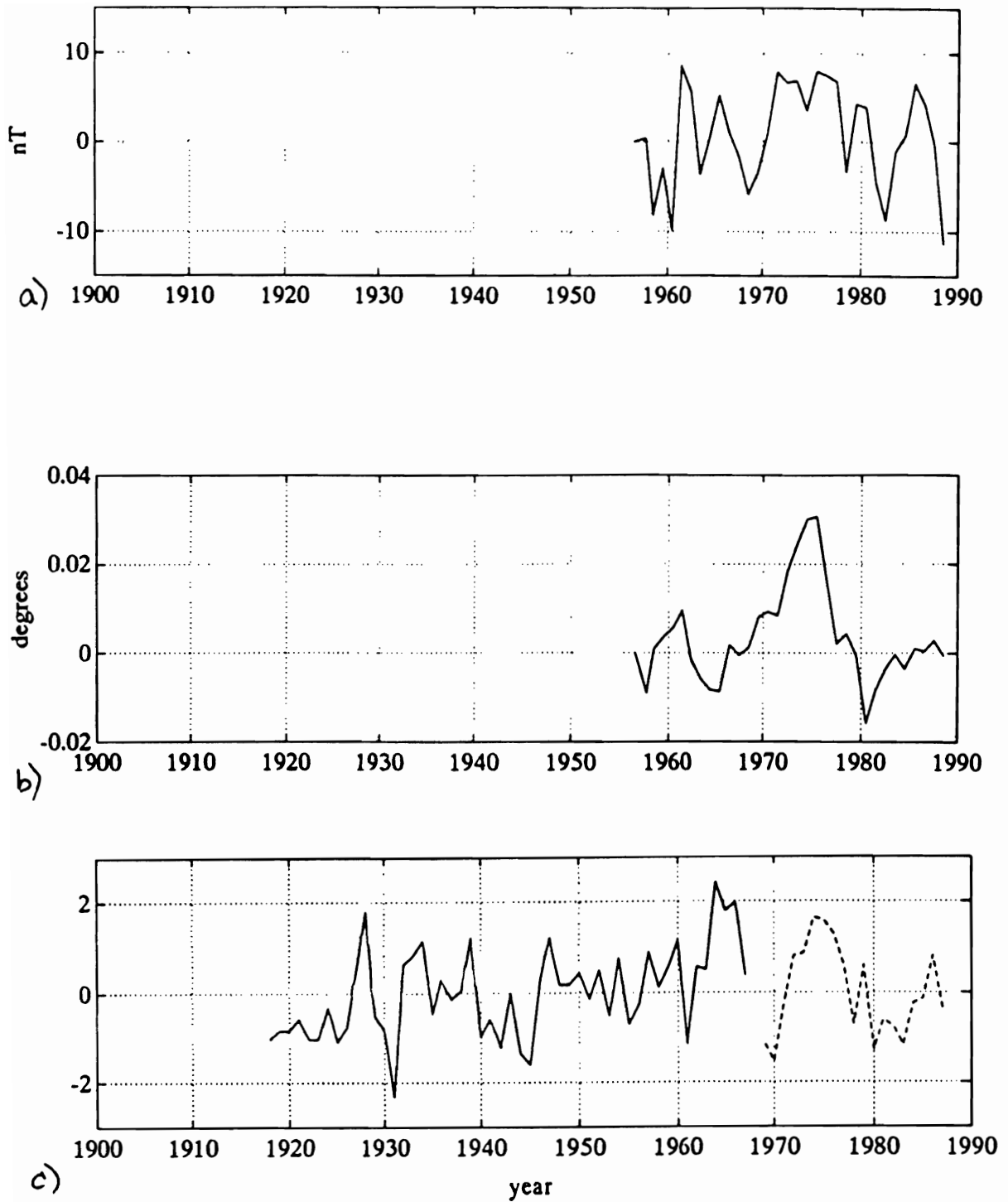


Figure 25: In (a) we see the magnetic intensity H , and in (b) the declination (both with a 10-year mean subtracted) recorded at Victoria, British Columbia. In (c) we present the composite time series of North American runoff. (See text for correlations.)

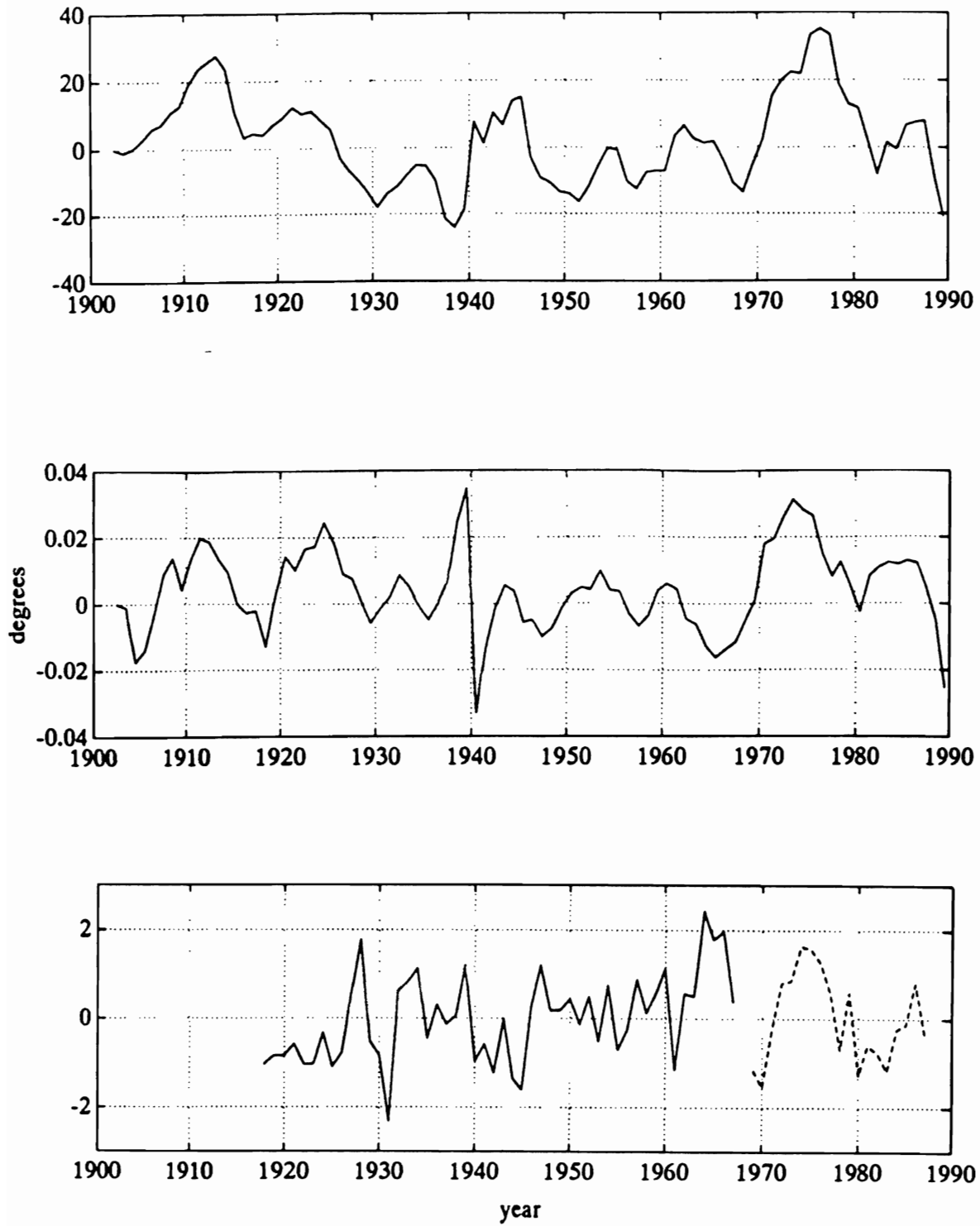


Figure 26: In (a) we see the magnetic intensity H , and in (b) the declination (both with a 10- year mean subtracted) recorded at Sitka, Alaska. In (c) we present the composite time series of North American runoff.

populated, high- latitude region. Of these conventional sources, we found that tree ring, ice and sediment cores may offer the greatest potential but it appears that their possible use as MacKenzie runoff proxies would require additional data collection.

We propose that existing geomagnetic data from permanent observatories and repeat stations may provide information about the MacKenzie runoff. Runoff and magnetic observations are related through the theory of motionally-induced electromagnetic fields in the sea (MIEFS) and the extent of MIEFS will depend principally on the salt transport of local and regional ocean currents. Since freshwater addition by rivers decrease the salinity of the ocean waters the salt transport (and observed MIEFS) may be reduced. (This assumes that the background ocean currents dominate buoyancy effects introduced by the river discharge.)

Often, however, (perhaps the situation we saw at Cambridge Bay was an example) river discharge may affect ocean salt transport in two different ways. The salinity of the water is decreased but the total volume transport is increased due to an increase in the buoyancy-driven (due to the river flux) component. These two effects change the total salinity transport in an opposing manner and in general, one does not clearly dominate the other. This makes the relationship between runoff and observed magnetic fluctuations less straight-forward. Hence, to relate the two, either some assumptions must be made concerning the runoff/buoyancy relationship, or, observations must be combined with simultaneous oceanographic measurements. Since Arctic oceanographic observations are historically as limited as the MacKenzie runoff records the last option is probably the least viable for our purposes.

In comparison with other directly-measured data in the Arctic the measurements of the geomagnetic field are geographically and historically abundant. Furthermore, techniques have been developed in the geological sciences that can create long geomagnetic reconstructions from ocean sediment cores. In this light, an elucidation of the MIEFS/runoff relationship seems very worthwhile.

It is worth mentioning finally that the magnetic records are vector sets containing extra directional information. Before this extra information can be fully exploited, the background ‘dipole’ field due to solid earth processes should be removed. This might be done by using magnetic data taken at observatories across the globe (with perhaps more weight given to the low-latitude stations where the horizontal ‘noise’ due to MIEFS is a minimum) to construct a standard dipole field for the earth. This base field could then be removed from the observations in the Arctic to elucidate the magnetic fields from MIEFS. Together with observations from repeat stations, a valuable description of large scale current systems in the Arctic might be obtained.

As we mentioned, the potential for extracting valuable climatic data from

the magnetic record is greatest in the Arctic. This is due to the the greater vertical component of the Earth's magnetic field at the poles, the great uniformity in arctic water temerature, and the great amount of freshwater runoff into the Arctic. Also, since oceanic and atmospheric data in the Arctic is historically sparse, the information pertaining to runoff (as well as other processes) that can be distilled from the magnetic records would be especially valuable.

5 Acknowledgements

This work was supported through grants (awarded to L.A. Mysak) from the Canadian Natural Sciences and Engineering Research Council, the Atmospheric Environment Service, and the U.S. Office of Naval Research. The author wishes to thank the following researchers for their helpful comments and suggestions: Rosanne D'Arrigo, John Weaver, D.B. Fissel, D.A. Fisher, M.A. Lapointe, Philip Marsh, Susan McLean, and Dave Holland.

6 References

Aagaard, K. and E.C. Carmack (1989) The Role of Sea Ice and Other Fresh Water in the Arctic Circulation. *Journal of Geophysical Research*, 94 (C10): 14485-14498.

Bradley, R.S. (1985) Quaternary Paleoclimatology. Allen and Unwin, Winchester, Mass, USA.

Cattle, H. (1985) Diverting Soviet Rivers: Some Possible Repercussions for the Arctic Ocean. *Polar Record*, 22(140): 485-498.

Coachman, L.K. and K. Aagaard (1988) Transports Through the Bering Strait: Annual and Interannual Variability. *Journal of Geophysical Research*, 93 (C12): 15,535-15539.

Filloux, J.H. (1987) Instrumentation and Experimental Methods for Oceanic Studies. In: *Geomagnetism Volume I* J.A. Jacobs, editor, Academic Press, San Diego.

Fisher, D.A. and R.M. Koerner (1983) Ice Core Study: A Climatic Link between the Past, Present and Future. In: *Climatic Change in Canada 3*, C.R. Harington, Editor; National Museum of Natural Sciences, Ottawa.

Fissel, D.B. and H. Melling (1990) Internannual Variability of Oceanographic Conditions in the Southeastern Beaufort Sea. Canadian Contractor Report of Hydrography and Ocean Sciences No. 35, 102 pages, (plus 6 microfiche).

Fritz, H. C. (1991) *Reconstructing Large-scale Climatic Patterns from Tree-Ring Data*. University of Arizona Press, Tucson, 286 pages.

Garfinkel, H. L. and L. B. Brubaker (1980) Modern Climate-Tree-Growth Relationships and Reconstruction in sub-Arctic Alaska. *Nature* Vol. 286: 872-873.

Hirst, S. M., M. Miles, S.P. Blachut, L.A. Goulet, and R.E. Taylor (1987) Quantitative Synthesis of the MacKenzie Delta Ecosystems, Report prepared for: Inland Waters Directorate, Environment Canada.

Ikeda, M. (1990) Decadal Oscillations of the Air-Ice- Ocean System in the Northern Hemisphere. *Atmosphere-Ocean*, 28 (1): 106-139.

Kelly, P.M., C.M. Goodess and B.S.G. Cherry (1987) The Interpretation of the Icelandic Sea Ice Record. *Journal of Geophysical Research*, 92: 10835-10843.

Koerner, R.M. (1977) Devon Island Ice Cap; Cores Stratigraphy and Paleoclimate. *Science*, 196:15-18.

Longuet-Higgins, M.S., M.E. Stern and H. Stommel (1954) The Electrical Field Induced by Ocean Currents and Waves, with Applications to the Method of Towed Electrodes. Papers in Physical Oceanography and Meteorology. MIT and WHOI, Vol 13, No.1, Cambridge and Woods Hole, Massachusetts. 37 pages.

Malin, S. (1987) Historical Introduction to Geomagnetism. In: *Geomagnetism Volume I*, J.A. Jacobs, editor, Academic Press, San Diego.

Manabe, S. and R.J. Stouffer (1988) Two Stable Equilibria of a Coupled Ocean-Atmosphere Model. *Journal of Climate*, 1: 841-866

Markova, O.L. (1978) In *World Water Balance and Water Resources of the Earth*, Unesco Press, Paris, pp. 328-349. First published in Russian (1974).

Moodie, D.W. and A.J.W. Catchpole (1975) *Environmental Data from Historical Documents by Content Analysis*. Manitoba Geography Studies No.5, Department of Geography, University of Manitoba, Winnipeg. 119 pages.

Mysak, L. A. (1992) Decadal Scale Variability of Ice Cover and Climate in the Arctic Ocean and Greenland Sea. To appear in proceedings of the workshop on Decade to Century Time Scales of Natural Climate Variability, Irvine, California, National Academy Press.

Mysak, L. A. and D. K. Manak (1989) Arctic Sea- Ice Extent and Anomalies, 1953-1984. *Atmosphere-Ocean*, 27 (2) 376-405.

Mysak, L. A. and S.B. Power (1991) Greenland Sea Ice and Salinity Anomalies and Interdecadal Climate Variability. *Climatological Bulletin*, 25:81-91.

Mysak, L.A., D.K. Manak and R.F. Marsden (1990) Sea- Ice Anomalies Observed in the Greenland and Labrador Seas during 1901-1984 and their Relation to an Interdecadal Arctic Climate Cycle. *Climate Dynamics*, 5:111-133

Newitt, L.R., R.L. Coles and J.F. Clark (1985) Canadian Magnetic Repeat Stations 1962-1983: Instruments, Procedures and Observations. Geomagnetic Series No. 29, Energy Mines and Resources Canada, Ottawa.

Ostrem, G. and M. Brugman (1991) Glacier Mass-Balance Measurements, NHRI Science Report No. 4, Inland Waters Directorate, Environment Canada.

Sanford, T. B., (1971) Motionally Induced Electric Fields in the Sea. *Journal of Geophysical Research*, Vol. 76, No. 15: 3476-3493.

Stocker, T. F. and D. G. Wright (1991) Rapid Transitions of the Ocean's Deep Circulation Induced by Changes in Surface Water Fluxes. *Nature*, 351: 729-732

Stockton, C. W. and H. C. Fritts (1973) Long- Term Reconstruction of Water Level Changes for Lake Athabasca by Analysis of Tree Rings, *Water Resources Bulletin*, American Water Resources Association vol. 9, no.5.

Thomas, K. (1965) Climatic Trends on the Canadian Prairies, in: Water and Climate. Water Studies Inst. Report No. 2, Saskatoon, Sask., pp. 21-45.

Wangness, R. K., (1986) Electromagnetic Fields, 2nd Edition, John Wiley and Sons, N.Y., 587 pp.

Weaver, A. J. and T.M.C. Hughes (1992) Stability and Variability of the Thermo-haline Circulation and its link to Climate. *Center for Climate and Global Change Research*, Report No. 92-5, McGill University.